### Title

Cell-specific Deletion of NLRP3 Inflammasome Identifies Myeloid Cells as Key Drivers of Liver Inflammation and Fibrosis in Murine Steatohepatitis




### Journal

Cellular and Molecular Gastroenterology and Hepatology, 14(4)

### ISSN

2352-345X



### Authors

Kaufmann, Benedikt
Kui, Lin
Reca, Agustina
et al.



### Publication Date

2022

### DOI

10.1016/j.jcmgh.2022.06.007

Peer reviewed

cmgh
CELLULAR AND MOLECULAR GASTROENTEROLOGY AND HEPATOLOGY

ORIGINAL RESEARCH

# Cell-specific Deletion of NLRP3 Inflammasome Identifies Myeloid Cells as Key Drivers of Liver Inflammation and Fibrosis in Murine Steatohepatitis

Benedikt Kaufmann,[1,2] Lin Kui,[1] Agustina Reca,[1] Aleksandra Leszczynska,[1] Andrea D. Kim,[1] Laela M. Booshehri,[1] Alexander Wree,[3] Helmut Friess,[2] Daniel Hartmann,[2] Lori Broderick,[1] Hal M. Hoffman,[1] and Ariel E. Feldstein[1]

*[1]Department of Pediatrics, University of California San Diego, La Jolla, California; [2]Department of Surgery, TUM School of Medicine, Klinikum Rechts der Isar, Technical University of Munich, Munich, Germany; and [3]Charité, Campus Virchow Klinikum and Charité, Campus Mitte, Department of Hepatology and Gastroenterology, Universitätsmedizin Berlin, Berlin, Germany*

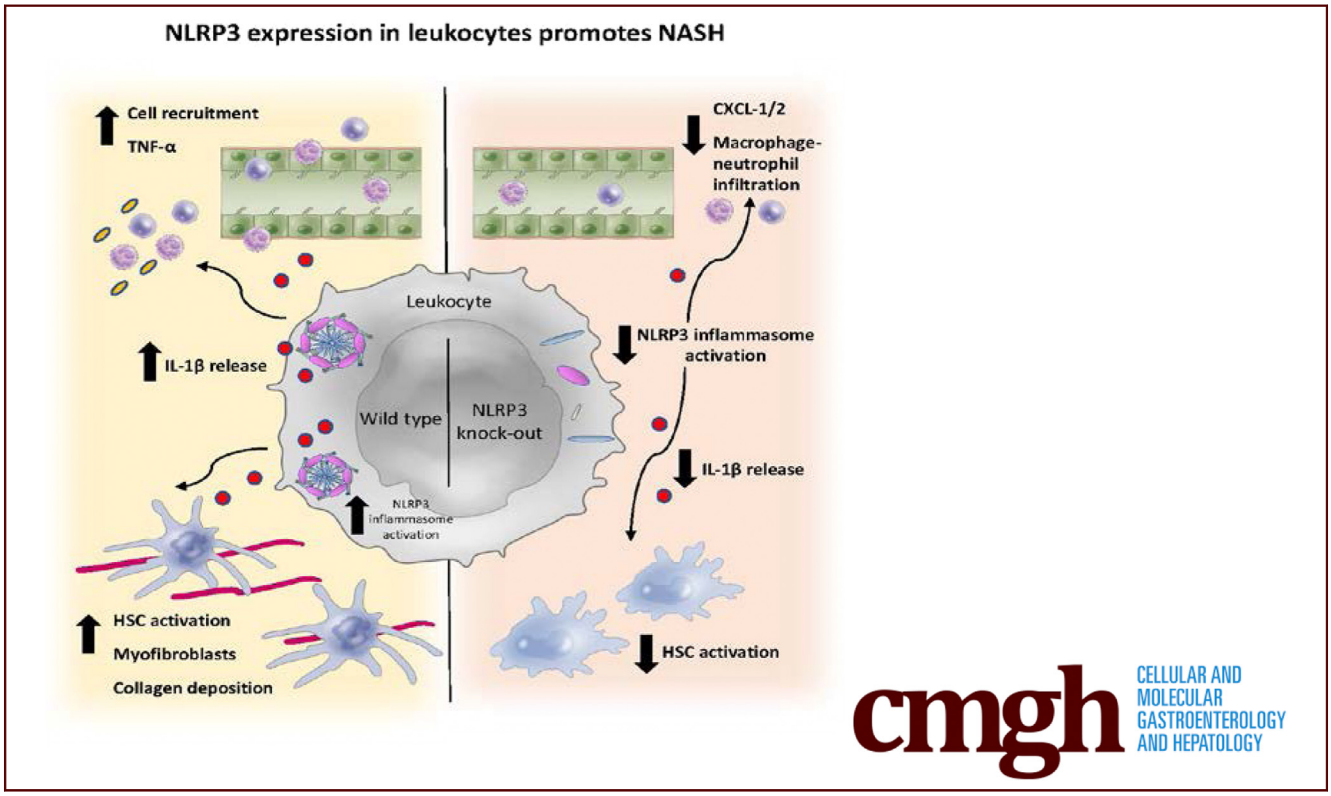


## SUMMARY

The NLRP3 inflammasome, a platform for caspase-1 activation and release of interleukin 1$\beta$, is important in the induction of hepatic inflammation and fibrosis. In this study, we demonstrate that NLRP3 inflammasome activation in myeloid cells is crucial for the progression of nonalcoholic fatty liver disease to fibrotic nonacoholic steatohepatitis.

**BACKGROUND & AIMS:** Nonalcoholic fatty liver disease (NAFLD) is the leading cause of chronic liver disease worldwide. The NLRP3 inflammasome, a platform for caspase-1 activation and release of interleukin 1$\beta$, is increasingly recognized in the induction of inflammation and liver fibrosis during NAFLD. However, the cell-specific contribution of NLRP3 inflammasome activation in NAFLD remains unknown.

**METHODS:** To investigate the role of NLRP3 inflammasome activation in hepatocytes, hepatic stellate cells (HSCs) and myeloid cells, a conditional Nlrp3 knock-out mouse was generated and bred to cell-specific Cre mice. Both acute and chronic liver injury models were used: lipopolysaccharide/adenosine-triphosphate to induce in vivo NLRP3 activation, choline-deficient, L-amino acid-defined high-fat diet, and Western-type diet to induce fibrotic nonalcoholic steatohepatitis (NASH). In vitro co-culture studies were performed to dissect the crosstalk between myeloid cells and HSCs.

**RESULTS:** Myeloid-specific deletion of Nlrp3 blunted the systemic and hepatic increase in interleukin 1$\beta$ induced by lipopolysaccharide/adenosine-triphosphate injection. In the

choline-deficient, L-amino acid-defined high-fat diet model of fibrotic NASH, myeloid-specific Nlrp3 knock-out but not hepatocyte- or HSC-specific knock-out mice showed significant reduction in inflammation independent of steatosis development. Moreover, myeloid-specific Nlrp3 knock-out mice showed ameliorated liver fibrosis and decreased HSC activation. These results were validated in the Western-type diet model. In vitro co-cultured studies with human cell lines demonstrated that HSC can be activated by inflammasome stimulation in monocytes, and this effect was significantly reduced if NLRP3 was downregulated in monocytes.

**CONCLUSIONS:** The study provides new insights in the cell-specific role of NLRP3 in liver inflammation and fibrosis. NLRP3 inflammasome activation in myeloid cells was identified as crucial for the progression of NAFLD to fibrotic NASH. These results may have implications for the development of cell-specific strategies for modulation of NLRP3 activation for treatment of fibrotic NASH. *(Cell Mol Gastroenterol Hepatol 2022;14:751–767; https://doi.org/10.1016/j.jcmgh.2022.06.007)*

*Keywords:* Fibrogenesis; Inflammasome; Liver Inflammation; NLR Family Pyrin Domain Containing 3; Nonalcoholic Fatty Liver Disease.

Nonalcoholic fatty liver disease (NAFLD) is now the leading cause of chronic liver disease worldwide.[1] Progressive stages of NAFLD, associated with the presence of liver fibrosis, translate into clinically relevant complications such as cirrhosis, hepatocellular carcinoma, and an increase in liver-related and overall mortality.[2] NAFLD refers to a spectrum of histological abnormalities, with the hallmark of excessive fat accumulation in the liver. Multiple cellular and molecular mechanisms are involved in the transition from simple steatosis to more severe stages of NAFLD, including nonalcoholic steatohepatitis (NASH), characterized by steatosis, inflammation, hepatocellular injury, and fibrosis.[3] Although the pathogenesis of NAFLD and its advanced stage, NASH, continue to be explored, emerging evidence has shown an important role for NLRP3 inflammasome-driven inflammation.[4,5]

Inflammasomes are multi-protein complexes identified in both immune and nonimmune cells that release pro-inflammatory cytokines in response to a wide range of stimuli, including pathogen- and damage-associated molecular patterns.[6] The NLRP3 inflammasome, a platform for caspase-1 activation and release of interleukin 1$\beta$ (IL-1$\beta$), has been increasingly recognized in the induction of sterile inflammation, hepatocyte damage, cellular death, and liver fibrosis.[7-11] However, the contribution of cell-specific NLRP3 activation in NAFLD pathogenesis remains unknown.[12] Knock-in murine models have suggested that global, and to a lesser extent myeloid-specific NLRP3 inflammasome activation, results in severe liver inflammation and fibrosis.[13,14] Notably, constitutive activation of NLRP3 resulted in hepatic neutrophilic infiltration, hepatic stellate cell (HSC) activation with collagen deposition, and pyroptotic hepatocyte cell death.[13,15] Hepatocyte-specific NLRP3 inflammasome activation in this knock-in model was further shown to activate HSCs and to promote liver fibrosis via secretion of inflammasome complexes into the extracellular space.[16] In parallel, global *Nlrp3* knockout mice in choline-deficient, L-amino acid-defined induced NASH were protected from hepatomegaly, liver injury, and fibrosis with reduced hepatocyte pyroptosis and inflammatory markers.[8] Not only it is important to explore which cells are responsible for NLRP3 mediated inflammation and fibrosis, but it is also essential to understand the influence NLRP3 has on cellular crosstalk. The dynamic interplay between organs as well as recruited and resident cells is increasingly recognized as a determinant factor in the setting of chronic inflammation.[3,17] Neutrophils, traditionally seen as protagonists of inflammation, have been shown to influence cellular function and phenotype.[18] Together, these studies suggest a key role for cell-cell crosstalk in inflammatory metabolic and liver disease, but the individual cell-specific contributions within the liver and from recruited cells have not been previously investigated.[19,20]

In the present study, we generated a novel, conditional *Nlrp3* knock-out murine model to dissect the cell-specific role of NLRP3 in the development and progression of NAFLD. In contrast to our prior gain-of-function approach, the use of loss-of-function Nlrp3 models permits the study of the role of NLRP3 inflammasome-driven inflammation specifically during NAFLD development and progression, where inflammasome activation occurs as part of the pathogenic response. Abolishing NLRP3 inflammasome activity in a cell-specific manner further allowed us to investigate the link between NLRP3 and different inflammatory and fibrogenic pathways. Here, we aimed to explore the contribution of NLRP3 in hepatocytes, HSCs, and myeloid cells in NLRP3-mediated inflammation, fibrogenesis, and disease severity, with the goal of understanding the intercellular communication that takes place during NAFLD development and the influence of NLRP3 activation.[19,20]

## Results

### NLRP3-mediated Systemic and Liver Inflammation is Driven by Myeloid Lineage Cells

NLRP3 inflammasome activation is a key driver of liver inflammation.[3] The NLRP3 inflammasome is expressed in several cell types in the liver and elsewhere.[13,14,16] However, the role of NLRP3 activation in specific cell types in the pathogenesis of liver diseases is unknown. We hypothesized that NLRP3 expression in myeloid lineage cells is the key

***Abbreviations used in this paper:*** **Alb, albumin; ALT, alanine transaminase; ATP, adenosine-triphosphate; BSA, bovine serum albumin; CDAA-HFAT, choline-deficient, L-amino acid-defined high-fat diet; ELISA, enzyme-linked immunosorbent assay; H&E, hematoxylin and eosin; HSC, hepatic stellate cell; IL-1$\beta$, interleukin 1$\beta$; LPS, lipopolysaccharide; LRAT, lecithin retinol acyltransferase; Lyz, lysozyme; NAFLD, nonalcoholic fatty liver disease; NASH, nonalcoholic steatohepatitis; qPCR, quantitative polymerase chain reaction; SMA, smooth muscle actin; TGF, transforming growth factor; TNF, tumor necrosis factor; TUNEL, terminal deoxynucleotidyl transferase dUTP nick-end labeling.**

**Most current article**



2352-345X
https://doi.org/10.1016/j.jcmgh.2022.06.007

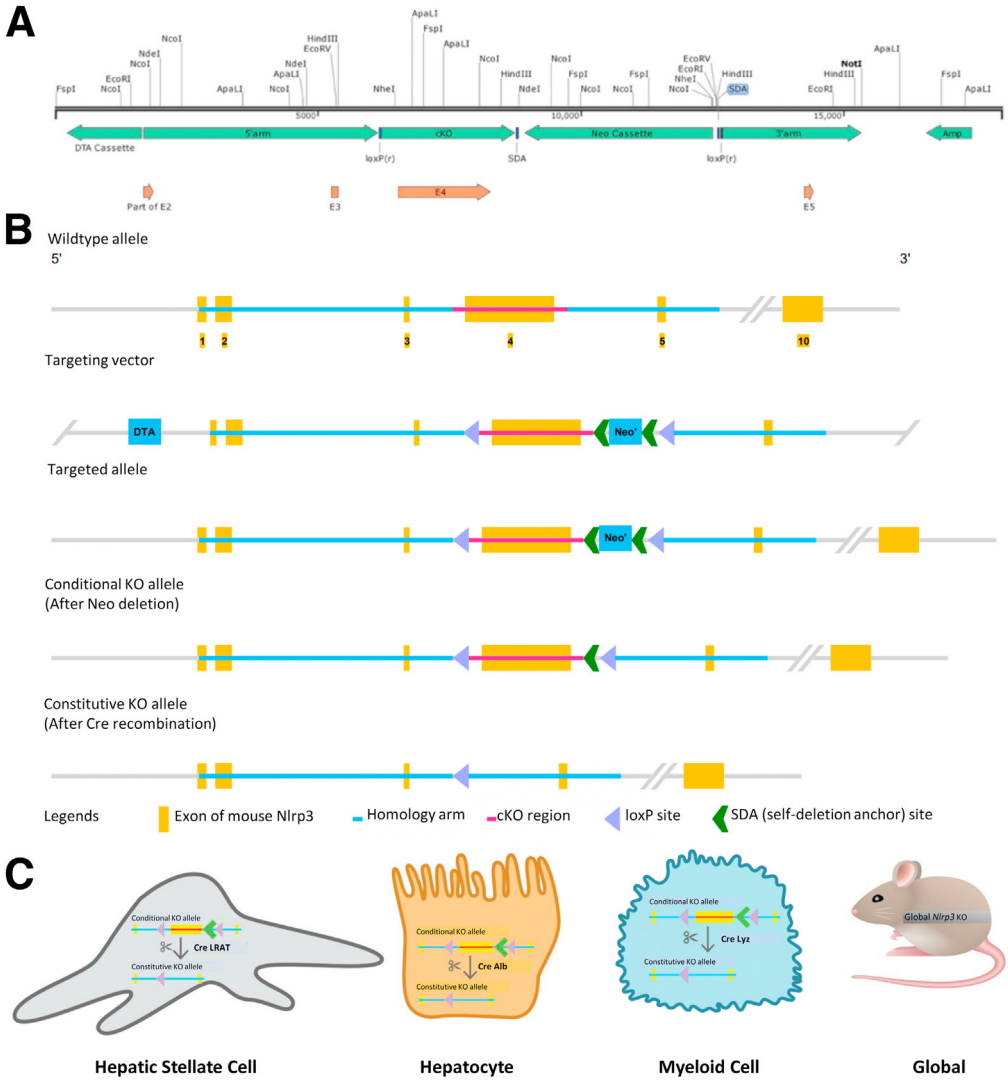


**Figure 1. Generation of *Nlrp3* conditional knockout mouse.** To investigate the cell-specific role of NLRP3 in liver diseases, a *Nlrp3* conditional knockout mouse model was generated. *A*, Restriction enzyme map of *Nlrp3* genomic region of interest. Exon 4 was selected as conditional knockout region because deletion of this region results in the loss of function of mouse NLRP3. *B*, Strategy for development of *Nlrp3* conditional knockout (cKO). A linearized vector was engineered made up of mouse genomic fragments containing homology arms and the conditional knockout region amplified from Bacterial Artificial Chromosome clone and sequentially assembled into a targeting vector together with recombination sites and selection markers. In the targeting vector, the Neo cassette was flanked by self-deletion anchor sites. Diphtheria toxin A was used for negative selection. The linearized vector was transfected into C57BL/6 embryonic stem cells that afterwards were injected into C57BL/6 embryos and re-implanted into CD-1 pseudo-pregnant females. Founder animals were identified by their coat color, their germline transmission was confirmed by breeding with C57BL/6 females and subsequent genotyping of the offspring. The knockout allele is obtained after Cre-mediated recombination. *C*, Illustration of cell-specific conditional and global *Nlrp3* knockout mice used in this study. *Nlrp3* conditional knockout mice were bred to mice expressing Cre recombinase under the control of LRAT, Alb, or Lyz promoters. In addition, previously described global *Nlrp3* knockout mice were used.

driver of NLRP3 inflammasome-induced liver inflammation. To investigate the cell-specific contribution of NLRP3 inflammasome-driven disease, a conditional *Nlrp3* knockout mouse model was generated (Figure 1, *A*–*B*). Breeding *Nlrp3* conditional knockout mice to mice expressing Cre recombinase under the control of albumin (Alb), lecithin retinol acyltransferase (LRAT) or lysozyme (Lyz) promoters resulted in mice lacking *Nlrp3* expression in either hepatocytes, HSCs, or myeloid cells, respectively (Figure 1, *C*). There was no apparent baseline phenotype observed in any of these mice. To investigate the cell-specific contributions of each of these subsets to NLRP3 inflammasome-dependent liver pathology as well as systemic disease, a model of acute inflammation was performed (Figure 2, *A*). In this model, lipopolysaccharide (LPS) and adenosine 5′-triphosphate (ATP) are administered sequentially via intraperitoneal injection. LPS acts as a priming stimulus inducing increased expression of *Nlrp3* and pro-IL-1$\beta$, whereas ATP is a prototypical second signal that results in activation of the NLRP3 inflammasome complex, thereby inducing the

processing and release of mature IL-1$\beta$.[21] Analysis of circulating mature IL-1$\beta$ in serum as well as in peritoneal lavage fluid by enzyme-linked immunosorbent assay (ELISA) showed a significant downregulation of IL-1$\beta$ in the *Nlrp3* global knock-out, and in the myeloid-specific knock-out mice compared with LPS-treated control mice ($P < .001$ for both groups). Hepatocyte- or HSC-specific *Nlrp3* knock-out did not show a significant reduction in IL-1$\beta$ levels in

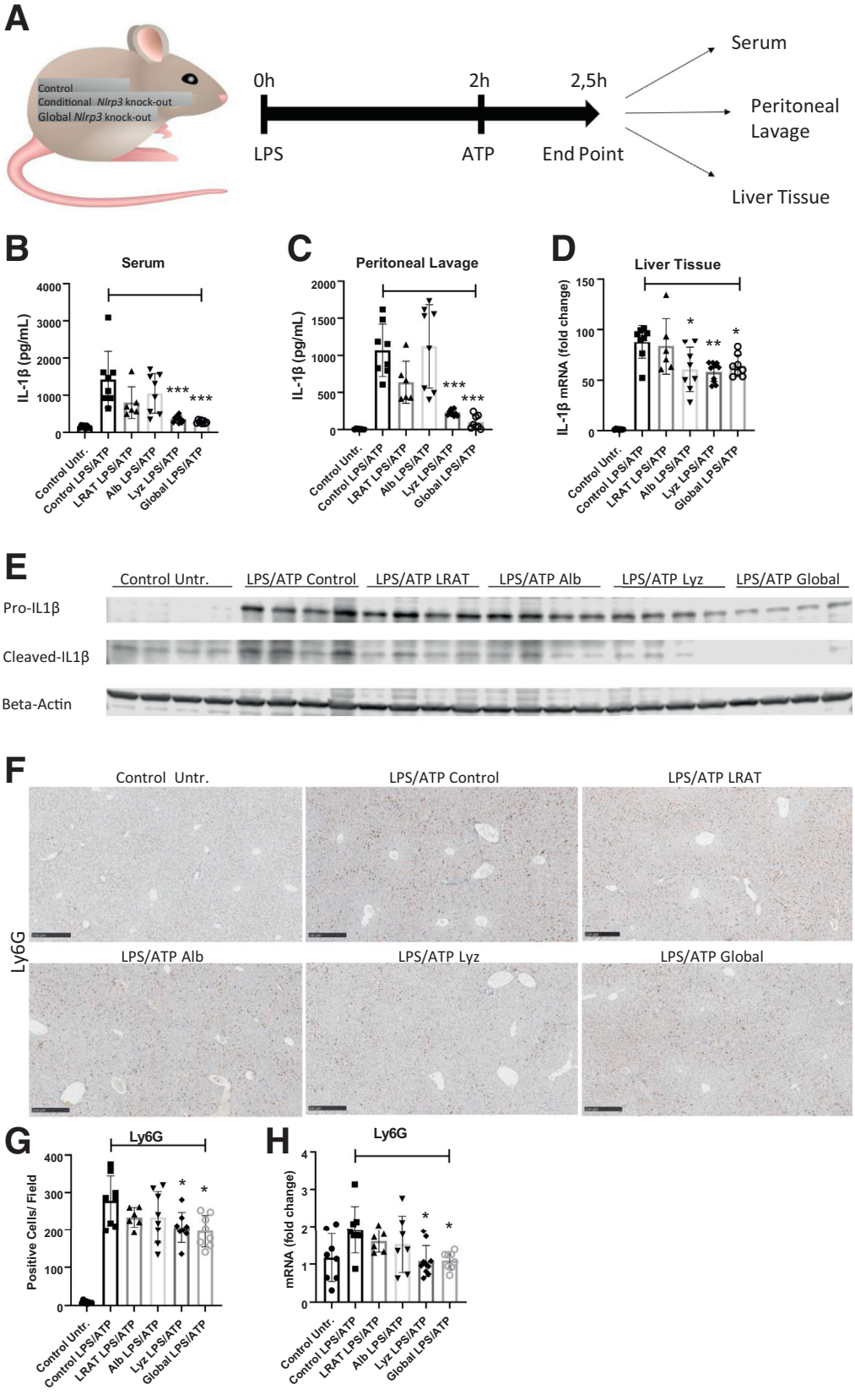

the serum or peritoneal lavage (Figure 2, *B–C*). Analysis of liver tissue revealed a significant downregulation of IL-1$\beta$ expression at the mRNA level in LPS-treated hepatocyte, myeloid-specific, and global knock-out compared with LPS-treated control mice (*Nlrp3*$^{-/-}$*-Alb-cre* p<0,05, *Nlrp3*$^{-/-}$*-Lyz-cre* $P < .01$; Global *Nlrp3*$^{-/-}$ $P < .05$) (Figure 2, *D*). Protein expression of both precursor and mature IL-1$\beta$ was primarily reduced in global knockout mice, and to lesser extent in myeloid-specific knock-out mice (Figure 2, *E*). These data suggest that acute, IL-1 mediated inflammatory liver disease is dependent on NLRP3 inflammasome activation in myeloid cells.

Neutrophil infiltration to the liver occurs at an early stage of NLRP3 inflammasome-triggered liver inflammation.[8,13] To investigate whether hepatic neutrophil infiltration was dependent on cell-specific NLRP3 expression, immunostaining of Ly6G was performed on whole liver tissue. Global and myeloid-specific *Nlrp3* knock-out mice had a significant reduction in infiltrating neutrophils into the liver (*Nlrp3*$^{-/-}$*-Lyz-cre*, $P < .05$; Global *Nlrp3*$^{-/-}$, $P < .05$), whereas hepatocyte- and HSC-specific Nlrp3 knock-out mice showed a similar degree of neutrophil infiltration compared with LPS/ATP-treated control mice (Figure 2, *F–G*). In addition, mRNA expression of Ly6G was decreased in global and myeloid-specific knock-out mice but not in hepatocyte- and HSC-specific *Nlrp3* knock-out mice compared with LPS/ATP-treated littermate controls (*Nlrp3*$^{-/-}$*- Lyz-cre*, $P < .05$; Global *Nlrp3*$^{-/-}$, $P < .05$) (Figure 2, *H*). These results demonstrate a key role for NLRP3 inflammasome activation in myeloid cells in promoting neutrophilic liver inflammation.

## *Selective Deletion of NLRP3 in Myeloid Cells Protects From Cell Death and Pro-inflammatory Cytokine Expression Triggered by Choline-deficient, L-amino Acid-defined High-fat Diet (CDAA-HFAT) Diet Independent Of Steatosis*

NLRP3 has an essential role in chronic liver disease, and especially in the development of NASH and fibrosis.[8] To analyze the role of cell-specific NLRP3 expression in NASH, *Nlrp3* conditional knock-out mice bred to myeloid-, HSC-, and hepatocyte-specific Cre mice and global *Nlrp3* knock out mice were given a CDAA-HFAT diet for 10 weeks, leading to an advanced stage of NASH and fibrosis. Hematoxylin and eosin (H&E) staining of livers revealed no differences in the degree of steatosis when comparing the different cell-specific and global *Nlrp3* knock-out groups with dietary control mice (Figure 3, *A*). In addition, liver weight, liver weight/body weight ratio, and serum alanine transaminase (ALT) levels did not show a significant difference when comparing the various *Nlrp3* knock-out groups and control group on diet (Figure 3, *C–D*). These results suggest that the initial insult of increased lipid accumulation and hepatocyte lipotoxicity induced by this diet occurs independently of NLRP3 activation. Beyond lipid accumulation, increased cell death along with pro-inflammatory cytokines and chemokines with subsequent recruitment of myeloid cells and development of inflammatory foci represent a fundamental pathophysiological feature of NASH with NLRP3 inflammasome activation being a proposed trigger.[11] We next evaluated the role of cell-specific NLRP3 expression in CDAA-HFAT diet-induced NASH. Pyroptosis, a form of programmed cell death dependent on caspase 1, was described to be crucial in the development of liver inflammation and fibrosis.[8,13,16] To assess programmed cell death in the liver, terminal deoxynucleotidyl transferase dUTP nick-end labeling (TUNEL) staining was performed. Liver tissue of mice on CDAA-HFAT diet showed a strong increase of TUNEL positivity compared with liver tissue of mice on chow diet. The livers of global and myeloid-specific knock-out mice revealed significant less TUNEL positivity compared with control mice on CDAA-HFAT diet, suggesting myeloid cells undergoing pyroptotic cell death (*Nlrp3*$^{-/-}$*-Lys-cre*, $P < .05$; Global *Nlrp3*$^{-/-}$, $P < .001$) (Figure 3, *B, E*). Expression of active caspase 1, the key protease in initiating pyroptotic cell death and the cleavage of pro-IL-1$\beta$, as well as the expression of the pro-inflammatory cytokines IL-1$\beta$ and tumor necrosis factor (TNF)-$\alpha$ were analyzed at the protein level. The active forms of caspase 1, IL-1$\beta$, and TNF-$\alpha$ were decreased in the livers of global and myeloid-specific knock-out mice compared with control mice (Casp1: *Nlrp3*$^{-/-}$*-Lys-cre*, $P < .05$; Global *Nlrp3*$^{-/-}$, $P < .05$; TNF-$\alpha$: *Nlrp3*$^{-/-}$*-Lys-cre*, $P < .05$; Global *Nlrp3*$^{-/-}$, $P < .05$) (Figure 3, *F–G*). HSC-specific knock-out mice did not show a difference, whereas hepatocyte-specific knock-out mice showed the tendency towards less expression of caspase 1, IL-1$\beta$, and TNF-$\alpha$ (Figure 3, *F–G*). These data suggest that CDAA-HFAT diet induces NLRP3 inflammasome activation in the liver is largely dependent on myeloid cells.

**Figure 2. NLRP3 mediated systemic and liver inflammation is driven by myeloid lineage cells.** *A*, Schematic for LPS/ATP induction of NLRP3 activation in vivo. *B–C*, Significant downregulation of IL-1$\beta$ release in serum and peritoneal lavage in response to NLRP3 activation in global, and to a slightly lesser extent myeloid-specific *Nlrp3* knock-out mice (*Nlrp3*$^{-/-}$*-Lyz-cre* p<0,001, Global *Nlrp3*$^{-/-}$, $P < .001$) compared with LPS/ATP-treated control mice analysed by ELISA was shown. Hepatocyte- and HSC-specific *Nlrp3* knock-out mice did not show a significant reduction in IL-1$\beta$ levels. *D*, Gene expression analysis of liver tissue revealed a significant downregulation of IL-1$\beta$ mRNA in hepatocyte-specific, myeloid-specific, and global Nlrp3 knock-out (*Nlrp3*$^{-/-}$*-Alb-cre*, $P < .05$; *Nlrp3*$^{-/-}$*-Lyz-cre*, $P < .01$; Global *Nlrp3*$^{-/-}$, $P < .05$) compared with control mice. *E*, Protein expression of both precursor and mature IL-1$\beta$ was primarily reduced in global *Nlrp3* knock-out mice and to lesser extent in myeloid-specific knock-out mice (n = 4 mice per genotype). *F–G*, Global and myeloid-specific *Nlrp3* knock-out mice showed a significant reduction in neutrophil infiltration to the liver (*Nlrp3*$^{-/-}$*-Lyz-cre*, $P < .05$; Global *Nlrp3*$^{-/-}$, $P < .05$) compared with LPS/ATP-treated control mice as measured by Ly6G staining. Hepatocyte- and HSC-specific *Nlrp3* knock-out mice did not show a significant difference in neutrophil infiltration compared with LPS/ATP-treated control mice. *H*, Expression of Ly6G mRNA was decreased in global and myeloid-specific *Nlrp3* knock-out mice (*Nlrp3*$^{-/-}$*-Lyz-cre*, $P < .05$; Global *Nlrp3*$^{-/-}$, $P < .05$), but not hepatocyte- and HSC-specific *Nlrp3* knock-out mice, compared with LPS/ATP-treated control mice. Representative images shown, bar indicates 250 $\mu$M, n $\geq$ 5 mice per genotype.

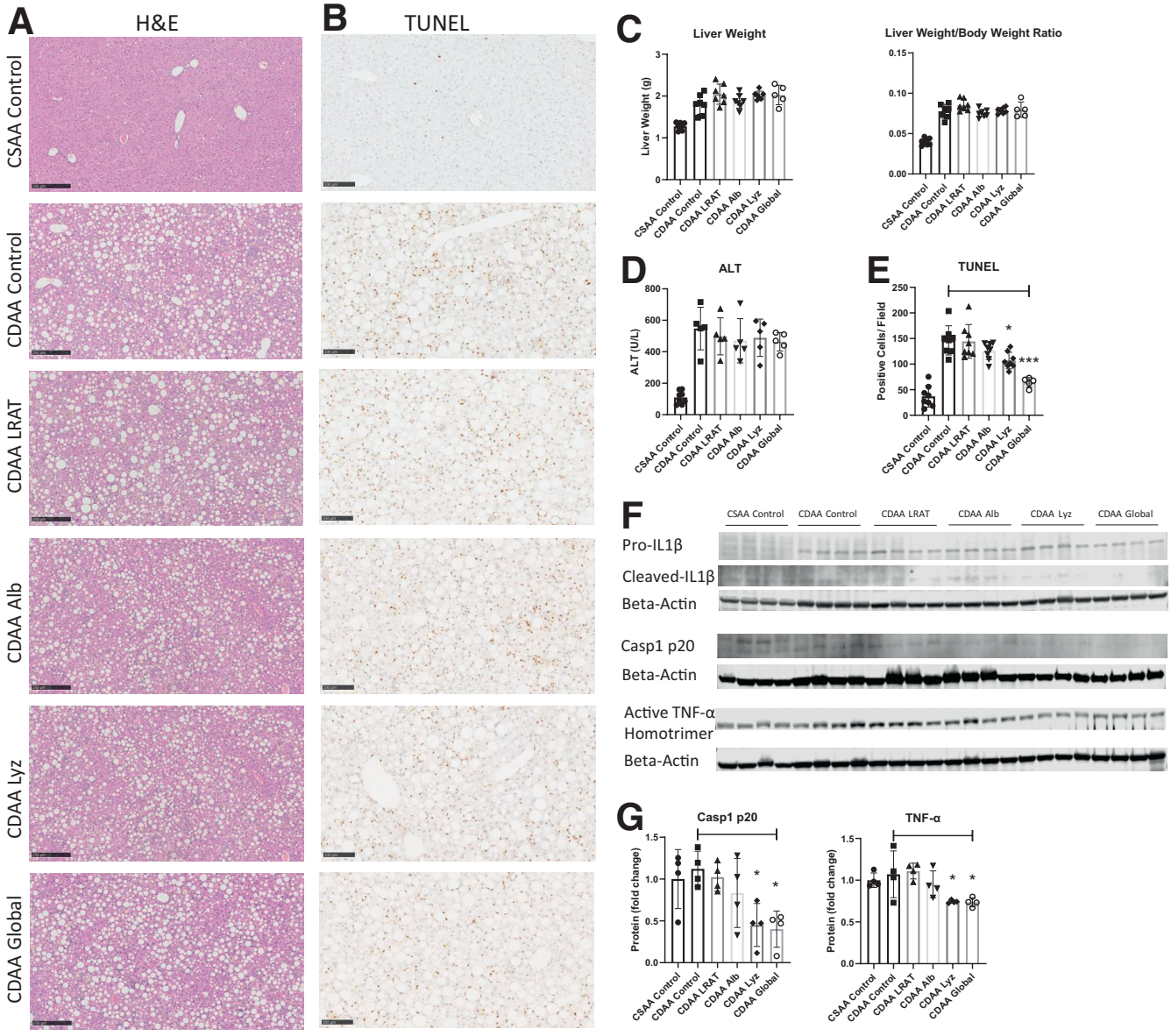


**Figure 3. Selective deletion of NLRP3 in myeloid cells protects from cell death and pro-inflammatory cytokine expression triggered by CDAA-HFAT diet independent of steatosis.** Mice were put on control or CDAA-HFAT diet for 10 weeks. *A*, H&E staining of livers showed no difference in the degree of steatosis when comparing the different knock-out groups with control group. *C–D*, Liver weight, liver weight/body weight ratio, and ALT level in serum did not show a significant difference. *B, E*, TUNEL positivity in livers of mice on CDAA-HFT diet was increased compared with mice on chow diet. Global and myeloid-specific knock-out mice show significant less TUNEL positivity compared with control mice ($Nlrp3^{-/-}$-Lys-cre, $P < .05$; Global $Nlrp3^{-/-}$, $P < .001$). *F–G*, Protein expression of the mature and active form of caspase1, IL-1$\beta$, and TNF-$\alpha$ were decreased in global and myeloid-specific Nlrp3 knock-out mice compared with control mice (Casp1: $Nlrp3^{-/-}$-Lyz-cre, $P < .05$; Global $Nlrp3^{-/-}$, $P < .05$; TNF-$\alpha$: $Nlrp3^{-/-}$-Lyz-cre, $P < .05$; Global $Nlrp3^{-/-}$, $P < .05$) (n = 4 mice per genotype). HSC-specific Nlrp3 knock-out mice did not show a difference, whereas hepatocyte-specific Nlrp3 knock-out mice showed a trend towards reduced expression of caspase-1, IL-1$\beta$, and TNF-$\alpha$. Representative images shown, H&E bar indicates 250 $\mu$M, TUNEL bar indicates 100 $\mu$M, n $\geq$ 5 mice per genotype.

## *NLRP3 Deletion in Myeloid Cells Protects From Immune Cell Changes in the Liver in CDAA-HFAT Diet-induced NASH*

Hepatic infiltration of neutrophils and macrophages after liver injury is important for an adequate inflammatory response. However, chronic liver injury leads to an imbalance of inflammatory homeostasis and promotes a shift towards a pro-inflammatory environment. Hereby, neutrophils play a key role in recruiting monocytes and orchestrating immune cell responses. To assess infiltration of myeloid-derived cells to the liver in response to high-fat diet, we performed immunostaining for CD11b (a marker for bone marrow-derived myeloid cells), Ly6G (a marker for neutrophils), and Ly6C (a marker for pro-inflammatory

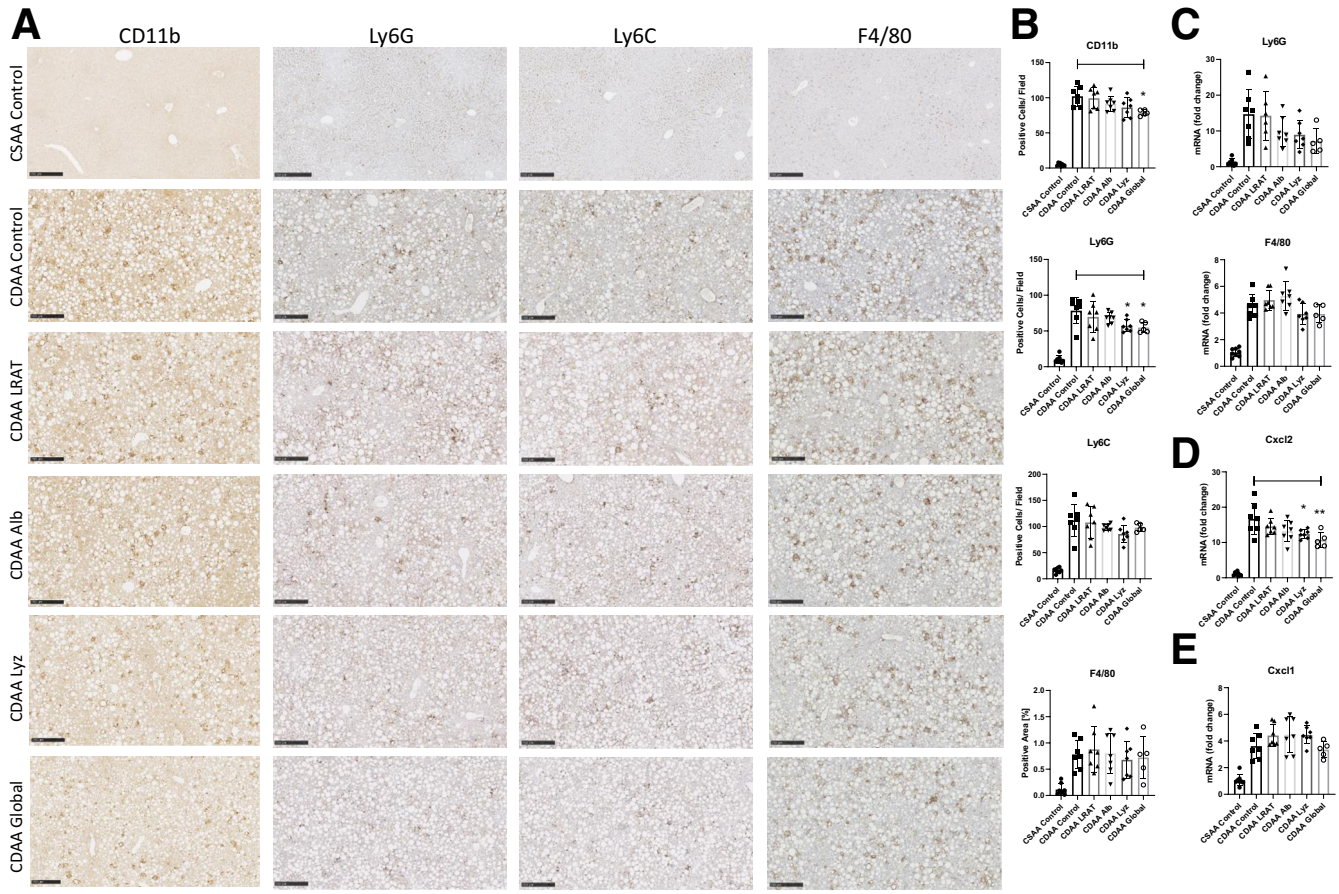


**Figure 4. NLRP3 deletion in myeloid cells protects from immune cell changes in the liver in CDAA-HFAT diet-induced NASH.** *A–B*, Quantification of CD11b staining demonstrated a significant decrease in CD11b+ myeloid cells in global *Nlrp3* knock-out mice (Global *Nlrp3*$^{-/-}$, $P < .05$), and a tendency towards reduced CD11b+ cells in myeloid-specific *Nlrp3* knock-out mice compared with control mice consuming a CDAA diet. *A–B*, Quantification of Ly6G staining demonstrated that neutrophil infiltration was significantly reduced in global and myeloid-specific *Nlrp3* knock-out mice (*Nlrp3*$^{-/-}$*-Lyz-cre*, $P < .05$; Global, $P < .05$) when compared with CDAA diet control mice. Foci of accumulated Ly6G+ neutrophils were also reduced in both global and myeloid-specific *Nlrp3* knock-out mice. *C*, Ly6G gene expression trended towards lower expression mainly in global and myeloid-specific *Nlrp3* knock-out mice, and to lesser extent in hepatocyte-specific *Nlrp3* knock-out mice, compared with diet-controlled mice. *A–B*, Staining for Ly6C revealed a trend towards a decrease in proinflammatory liver macrophages in global and myeloid-specific *Nlrp3* knock-out mice compared with control mice on a similar diet. *A–C*, Staining and mRNA gene expression of F4/80 did not show a difference between the various knock-out and CDAA control groups. *D*, *Cxcl2* gene expression was significantly downregulated in both global and myeloid-specific but not hepatocyte- and HSC-specific *Nlrp3* knock-out mice when compared with control mice (*Nlrp3*$^{-/-}$*-Lyz-cre*, $P < .05$; Global *Nlrp3*$^{-/-}$, $P < .01$). *E*, Gene expression of *Cxcl1* did not show a difference between the groups. Representative images shown, bar indicates 250 $\mu$M, n $\geq$ 5 mice per genotype.

macrophages). For the assessment of Kupffer cells, the hepatic resident macrophages, staining of F4/80 was performed. CD11b staining revealed a significant decrease in myeloid cell numbers in the liver in global *Nlrp3* knock-out mice, and a trend towards fewer CD11b+ cells in myeloid-specific knock-out mice (Global *Nlrp3*$^{-/-}$ $P < .05$) (Figure 4, *A–B*). Evaluation of Ly6G staining demonstrated that neutrophil infiltration was significantly reduced in global and myeloid-specific *Nlrp3* knock-out mice when compared with control mice (*Nlrp3*$^{-/-}$-Lyz-cre, $P < .05$; Global *Nlrp3*$^{-/-}$, $P < .05$). Foci of accumulated neutrophils were also reduced in both global- and myeloid-specific knock-out mice (Figure 4, *A–B*). Hepatocyte- and HSC-specific knock-out mice did not show a significant decrease, although both groups had marginally less neutrophil infiltration compared with control mice. Gene expression of Ly6G trended towards lower expression mainly in global- and myeloid-specific *Nlrp3* knock-out mice, and to a lesser extent in hepatocyte-specific knock-out mice compared with control mice, although this did not reach statistical significance (Figure 4, *C*). Staining for macrophage marker Ly6C revealed a slight decrease in proinflammatory macrophages in global and myeloid-specific *Nlrp3* knock-out mice compared with control mice (Figure 4, *A–B*). Quantification of staining and gene expression of F4/80 did not show a difference between *Nlrp3* knock-out and control groups (Figure 4, *A–C*). To further evaluate the recruitment of myeloid derived cells to the inflamed liver, we analyzed murine livers for expression of the chemoattractants *Cxcl1* and *Cxcl2*. Analysis of gene expression of *Cxcl2* demonstrated a significant

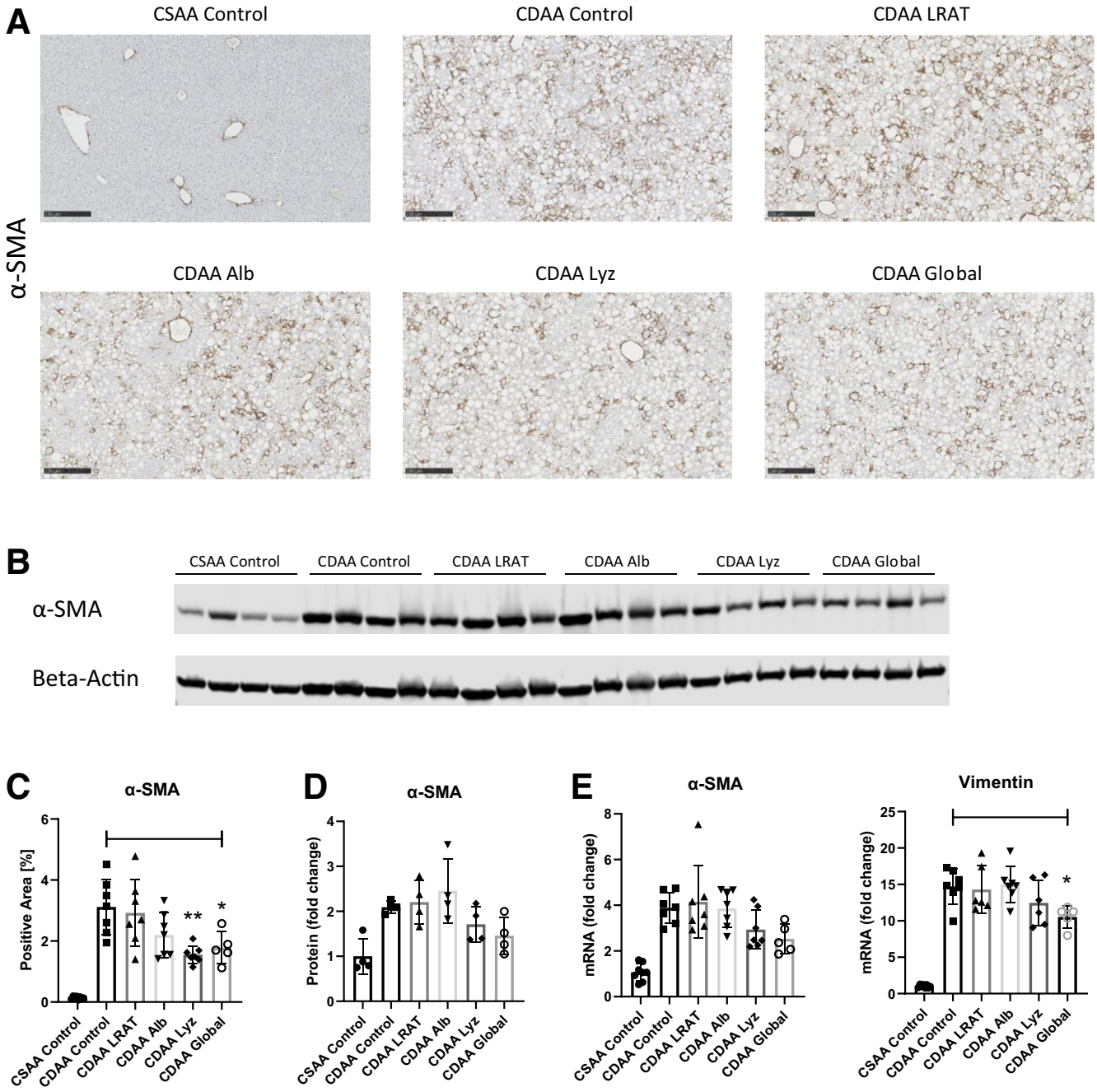


**Figure 5. Selective deletion of NLRP3 in myeloid cells decreases HSC activation.** *A, C*, Immunostaining of $\alpha$-SMA, a marker for activated HSCs, showed a lower expression in global and myeloid-specific *Nlrp3* knock-out mice (CDAA: *Nlrp3*$^{-/-}$-*Lyz-cre*, $P < .01$; Global, $P < .01$) compared with control mice consuming a CDAA diet. *B, D*, Protein expression of $\alpha$-SMA was decreased in global and myeloid-specific knock-out mice compared with control mice (n = 4). *E*, Gene expression of the $\alpha$-SMA gene *Acta2,* as well as vimentin, was reduced in global and to a lesser extent in myeloid-specific *Nlrp3* knock-out mice compared with control mice (*Nlrp3* Global, $P < .01$). Representative images shown, bar indicates 250 $\mu$M, n $\geq$ 5 mice per genotype.

downregulation of *Cxcl2* in both global and myeloid-specific *Nlrp3* knock-out mice, but not in hepatocyte- and HSC-specific Nlrp3 knock-out mice when comparing with control mice (*Nlrp3*$^{-/-}$-Lyz-cre, $P < .05$; Global *Nlrp3*$^{-/-}$, $P < .01$) (Figure 4, *D*). Gene expression of *Cxcl1* was similar within the different *Nlrp3* knock-out groups (Figure 4, *E*). Taken together, these data identify myeloid cells as the predominant cell type in the liver that drives pro-inflammatory cytokine and chemokine responses and infiltration with inflammatory neutrophils induced by the CDAA-HFAT dietary model in a process dependent on NLRP3-inflammasome activation.

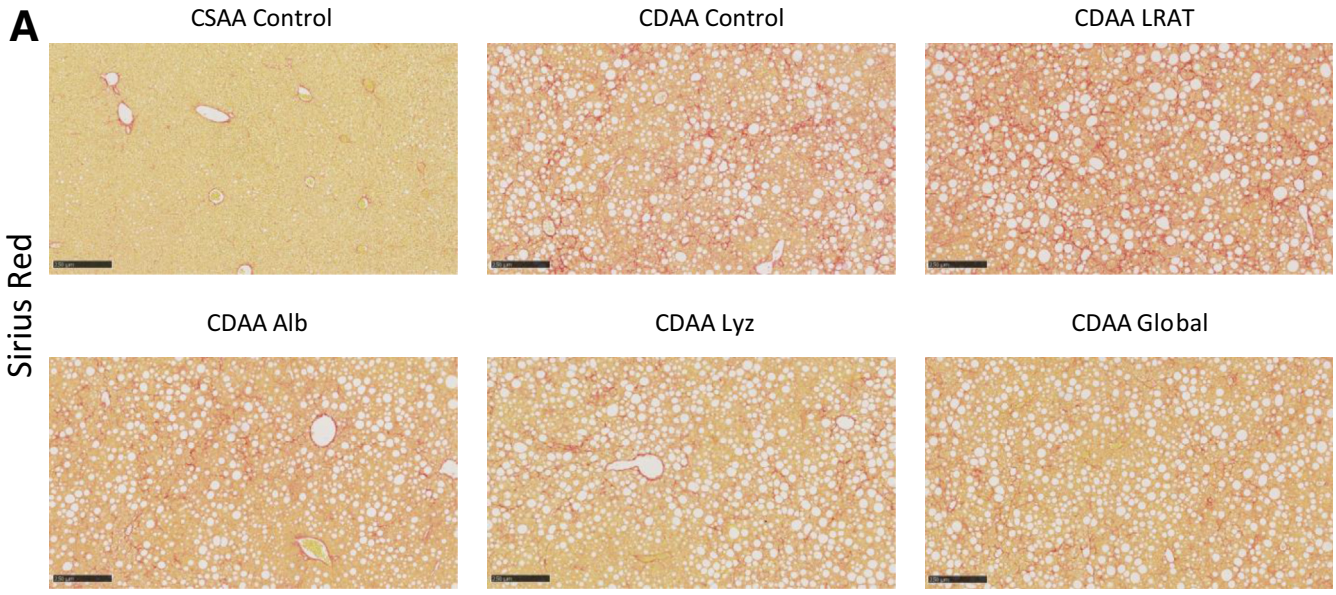
A
CSAA Control
CDAA Control
CDAA LRAT
Sirius Red
CDAA Alb
CDAA Lyz
CDAA Global

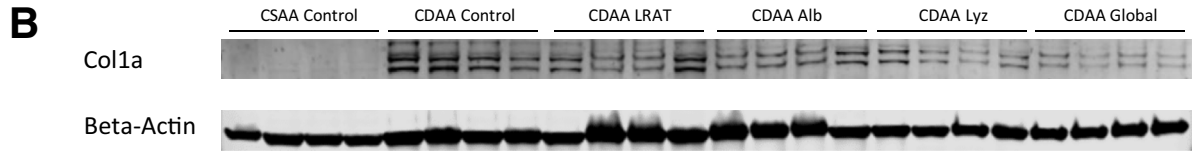
B
CSAA Control
CDAA Control
CDAA LRAT
CDAA Alb
CDAA Lyz
CDAA Global
Col1a
Beta-Actin

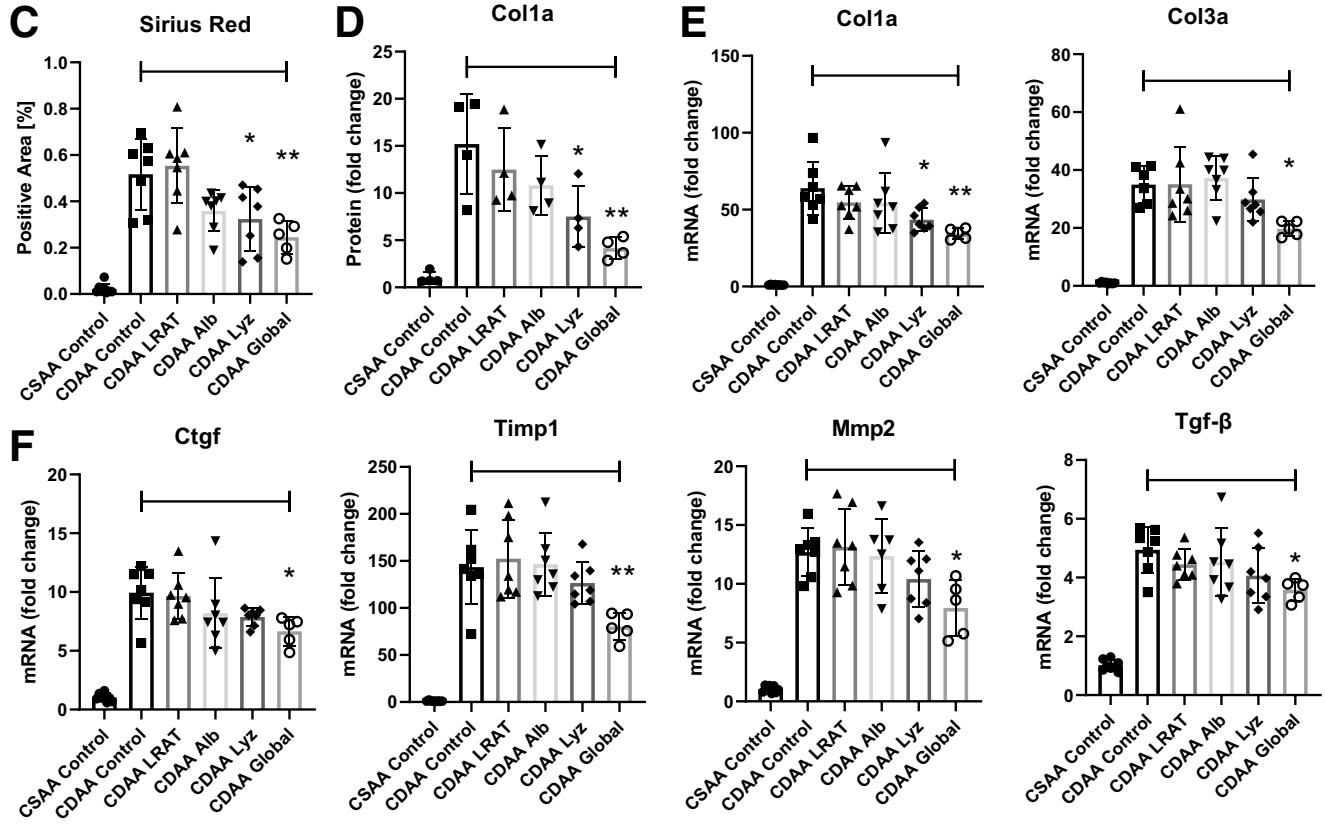
C
Sirius Red
Positive Area [%]
D
Col1a
Protein (fold change)
E
Col1a
Col3a
mRNA (fold change)
F
Ctgf
Timp1
Mmp2
Tgf-β
CSAA Control
CDAA Control
CDAA LRAT
CDAA Alb
CDAA Lyz
CDAA Global

## Selective Deletion of NLRP3 in Myeloid Cells Reveals Key Role of Crosstalk Between Inflammatory Cells and HSC in Regulation of HSC Phenotype and Activation

HSCs are the key effector cells in hepatic fibrogenesis. Once activated, HSCs transdifferentiate to myofibroblasts, resulting in collagen production, extracellular collagen deposition, and ultimately liver fibrosis. We previously demonstrated that hepatic NLRP3 expression triggered HSC activation.[16] To explore the contribution of specific cell types to diet induced activation of HSCs in liver tissue, we assessed expression of $\alpha$-smooth muscle actin (SMA) and vimentin as markers of HSC activation and proliferation. Immunostaining for $\alpha$-SMA in livers of global- and myeloid-specific *Nlrp3* knock-out mice revealed reduced expression of $\alpha$-SMA compared with control mice when administered a high-fat diet (*Nlrp3*$^{-/-}$-Lyz-cre, $P < .01$; Global *Nlrp3*$^{-/-}$, $P < .01$). Hepatocyte-specific knock-out mice showed a trend towards a lower expression of $\alpha$-SMA, whereas HSC-specific knock-out mice did not show a difference (Figure 5, *A, C*). Western blot further confirmed decreased protein expression of $\alpha$-SMA in global and myeloid-specific knock-out mice compared with control mice (Figure 5, *B, D*). Gene expression of $\alpha$-SMA and vimentin was reduced in global *Nlrp3* knock-out mice and to a lesser extent in myeloid-specific knock-out mice compared with control mice. In contrast, no difference in gene expression was observed in hepatocyte- and HSC-specific knock-out mice (Figure 5, *E*). These findings point to myeloid-derived cells as the key cell type by which NLRP3 activation modulates a pro-fibrotic HSC phenotype during NASH development.

## NLRP3 Deletion in Myeloid Cells Protects From Liver Fibrosis Induced by CDAA-HFAT Diet

Advanced stages of NASH are characterized by pathologic collagen deposition and fibrosis. NLRP3 has been shown to have an essential role in fibrogenesis.[8,13] However, the cell-specific contribution of NLRP3 on fibrosis remains unclear. Given the differential effects of cell specific changes in HSCs phenotype in the various knock-out mice, we next evaluated the role of NLRP3 in each cell type in liver fibrosis development induced by CDAA-HFAT diet. PicroSirius red staining to visualize collagen deposition demonstrated a significant reduction in fibrosis in global- and myeloid-specific knock-out mice (*Nlrp3*$^{-/-}$-Lyz-cre, $P < .05$; Global *Nlrp3*$^{-/-}$, $P < .01$) (Figure 6, *A, C*). Hepatocyte-specific knock-out mice showed a strong trend towards lower pathologic collagen deposition, whereas HSC-specific knock-out mice did not show a difference in collagen deposition compared with control mice (Figure 6, *A, C*). At the protein level, Western blot analysis confirmed decreased expression of collagen-1a in global and myeloid-specific knock-out mice, and a trend towards a lower expression in hepatocyte-specific knock-out mice when compared with control mice (*Nlrp3*$^{-/-}$-Lyz-cre, $P < .05$; Global *Nlrp3*$^{-/-}$, $P < .01$) (Figure 6, *B, D*). Expression of genes encoding collagen1a and collagen3a was decreased in global and myeloid-specific knock-out mice compared with control mice analyzed by quantitative polymerase chain reaction (qPCR) (*Nlrp3*$^{-/-}$-Lyz-cre, $P < .05$; Global *Nlrp3*$^{-/-}$, $P < .01$) (Figure 6, *E*). Expression of the pro-fibrogenetic genes *Ctgf*, *Timp1*, *Mmp2*, and *Tgf-β* was significantly lower in global knock-out mice (*Ctgf*, $P < .05$; *Timp1*, $P < .01$; *Mmp2*, $P < .05$; *Tgf-β*, $P < .05$). Myeloid-specific knock-out mice showed reduced expression of these genes compared with control mice but did not reach significance (Figure 6, *E*). These results confirm the pro-fibrotic role of NLRP3 during NASH development. Furthermore, it reveals myeloid-derived cells as the key cell type triggering diet-induced, NLRP3 inflammasome-dependent fibrogenesis.

## NLRP3 Deletion in Myeloid Cells Decreases HSC Activation and Fibrosis in a Western-type Diet-induced NASH

To further explore the role of NLRP3 in NASH, a second dietary murine model mimicking human NASH was used. Mice were placed on high-fat, fructose, and cholesterol diet and water supplemented with sucrose/fructose for 20 weeks. Similar to the findings in the CDAA-HFT diet model, degree of steatosis and liver weight/body weight ratio did not show a difference between the groups of mutant mice (Figure 7, *B, E*). Importantly, HSC activation was decreased in myeloid-specific Nlrp3 knock-out mice compared with control mice as shown by decreased expression of $\alpha$-SMA (*Nlrp3*$^{-/-}$*-Lyz-cre*, $P < .01$) (Figure 7, *C, F*). Furthermore, fibrosis was reduced in myeloid-specific Nlrp3 knock-out mice. PicroSirius staining revealed reduced collagen deposition in myeloid-specific Nlrp3 knock-out mice compared with control mice (*Nlrp3*$^{-/-}$*-Lyz-cre*, $P < .05$). These data highlight that myeloid-derived cells are the key cell type for

**Figure 6. (*See previous page*). NLRP3 deletion in myeloid cells protects from liver fibrosis induced by CDAA-HFAT diet.** *A, C*, Sirius red staining showed a significant reduction in pathological collagen deposition in global and myeloid-specific *Nlrp3* knock-out mice (*Nlrp3*$^{-/-}$*-Lyz-cre*, $P < .05$; Global *Nlrp3*$^{-/-}$, $P < .01$) compared with control mice. Hepatocyte-specific *Nlrp3* knock-out mice showed a strong trend towards reduced collagen deposition compared with control mice, whereas HSC-specific *Nlrp3* knock-out mice were unchanged. *B, D*, At the protein level, Western blot analysis confirmed decreased expression of collagen1a in global and myeloid-specific knock-out mice (*Nlrp3*$^{-/-}$*-Lyz-cre*, $P < .05$; Global, $P < .01$), with trends towards reduced expression in hepatocyte-specific *Nlrp3* knock-out mice when compared with control mice (n = 4). *E*, Expression of *Col1a* and *Col3a* were decreased in global and myeloid-specific Nlrp3 knockout mice (*Nlrp3*$^{-/-}$*-Lyz-cre*, $P < .05$; Global *Nlrp3*$^{-/-}$, $P < .01$) compared with control mice as analyzed by qPCR. *F*, Pro-fibrogenic genes such as *Ctgf, Timp1*, *Mmp2*, and *Tgf-β* were significantly less expressed in global *Nlrp3* knock-out mice (*Ctgf*, $P < .05$; *Timp1*, $P < .01$; *Mmp2*, $P < .05$; *Tgf-β*, $P < .05$) than control mice. Myeloid-specific *Nlrp3* knock-out mice showed a reduced expression of these genes compared to control mice on a similar diet. Representative images shown, bar indicates 250 $\mu$M, n $\geq$ 5 mice per genotype.

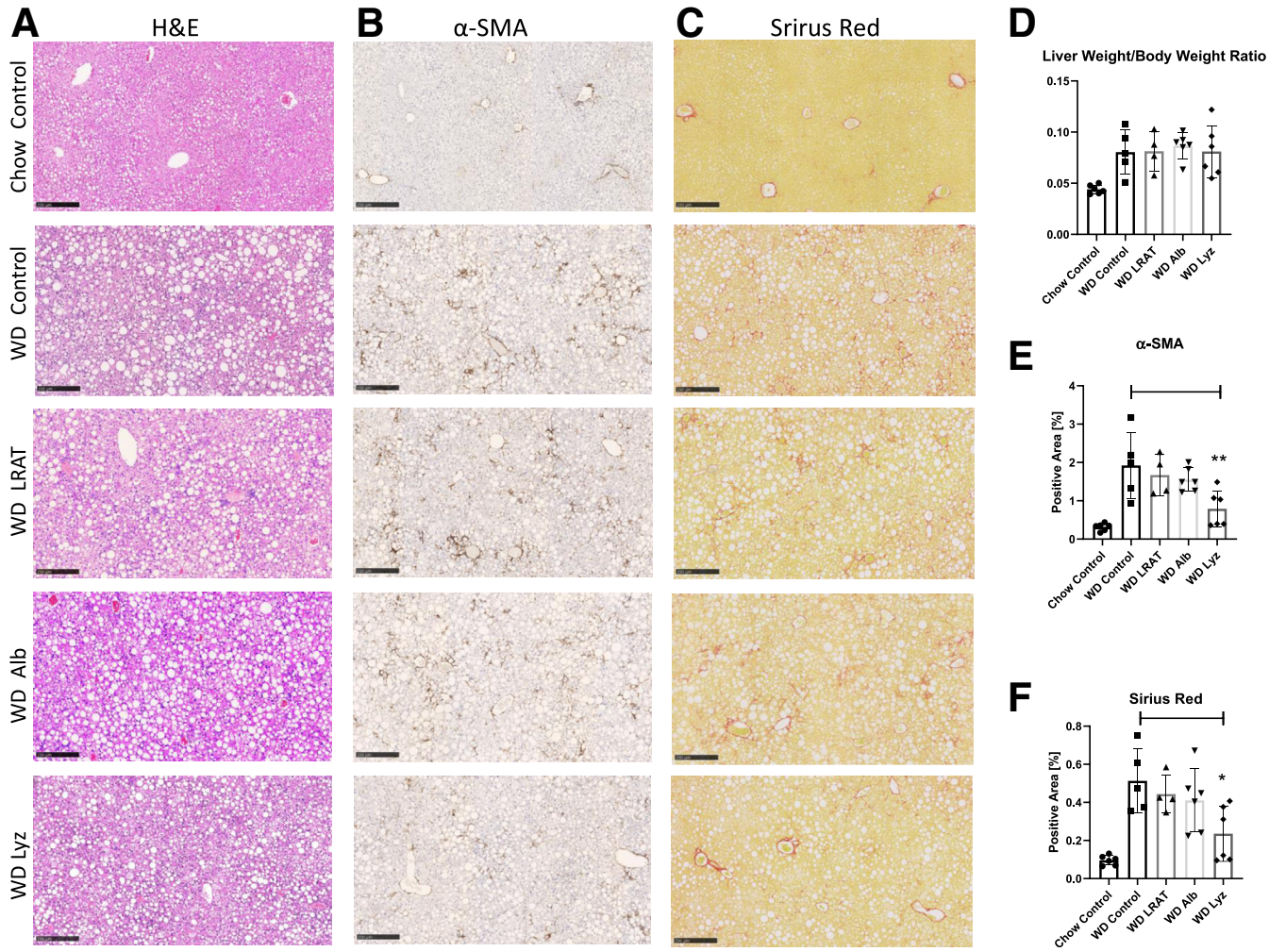


**Figure 7. NLRP3 deletion in myeloid cells decreases HSC activation and fibrosis induced by Western diet.** Mice were placed on a high fat, fructose, and cholesterol diet and water supplemented with sucrose/fructose. *A, D*, Mutant mice did not show a difference in degree of steatosis and liver weight/body weight ratio. *B, E*, Myeloid-specific Nlrp3 knock-out mice show decreased expression of $\alpha$-SMA compared with control mice (*Nlrp3*$^{-/-}$*-Lyz-cre*, $P < .01$). *C, F*, PicroSirius staining revealed reduced collagen deposition in myeloid-specific Nlrp3 knock-out mice (*Nlrp3*$^{-/-}$*-Lyz-cre*, $P < .05$). Representative images shown, bar indicates 250 $\mu$M, n $\geq$ 4 mice per genotype.

NLRP3 inflammasome-dependent HSC activation and fibrogenesis during NASH development.

### *NLRP3 Activation in Monocytes Modulates Transdifferentiation of HSCs Into Myofibroblast in Co-cultured in vitro Studies*

To explore the potential mechanisms involved in the protective effect found in the myeloid-specific NLRP3 KO on CDAA-HFAT-induced liver fibrosis, we performed in vitro co-culture studies. The human HSC cell line LX2 and human monocyte cell line THP-1, as well as the THP-1 NLRP3 knockdown cell line (THP1-NLRP3KD) were utilized in these studies to investigate the crosstalk between monocytes and HSCs. THP-1 or THP-1-NLRP3KD were grown in cell culture inserts and stimulated with LPS (1 $\mu$g/mL), washed, stimulated with nigericin (12.5 $\mu$M), and then co-cultured with LX-2 cells for 24 hours by placing the inserts containing THP-1 or THP-1-NLRP3KD in wells containing LX-2 cells at the bottom. (Figure 8, *A*). LX-2 cells activated with transforming growth factor (TGF)-$\beta$ (2.5 ng/mL) or incubated with nigericin alone were used as positive and negative controls, respectively. Co-culture of LX-2 with THP-1 that were stimulated with LPS and nigericin showed significantly increased mRNA expression of the HSC activation markers *Col1a*, *Ctgf*, *TGF-β*, *Timp1*, *Timp2*, and vimentin compared with LX-2 treated with nigericin only (*Col1a*, $P < .01$; *Ctgf*, $P < .05$; *Tgf-β*, $P < .05$; *Timp1*, $P < .001$; *Timp2*, $P < .05$; vimentin, $P < .01$) (Figure 8, *B*). There was no significant difference in gene expression between LX-2 co-cultured with LPS and nigericin-stimulated THP-1-NLRP3KD, and LX-2 treated with nigericin only or untreated LX-2. In contrast, LX-2 co-cultured with LPS and nigericin-stimulated THP-1-NLRP3KD revealed significantly reduced mRNA expression of HSC activation markers compared with LX-2 co-cultured with stimulated THP-1 (*Col1a*, $P < .01$; *Timp1*, $P < .001$; *Timp2*, $P < .01$) (Figure 8, *B*). LX-2 treated with TGF-$\beta$ as positive control

showed an increase of mRNA expression of HSC activation markers (*Col1a*, $P < .001$; *Ctgf*, $P < .001$; *Tgf-β*, $P < .05$; *Timp1*, $P < .001$), whereas nigericin treatment alone did not increase gene expression of these markers compared with untreated LX-2 (Figure 8, *B*). These data highlight that human HSC can be activated by inflammasome-stimulated monocytes, and this effect was significantly reduced if NLRP3 was downregulated in monocytes. The findings support a soluble factor crosstalk between monocytes and HSC contributing to the activation of HSC into myofibroblast collagen-producing cells, a central step in the development of fibrosis during NASH.

## Discussion

Recent studies identified a crucial role for the NLRP3 inflammasome in acute and chronic liver diseases including NASH, now the most common chronic liver disease globally.[7,8,13,20,22] Activation of the NLRP3 inflammasome and consequently caspase 1 leads to the release of IL-1β, and promotes secretion of pro-inflammatory cytokines, including TNF-α, which further enhance hepatic inflammation and fibrogenesis in the liver.[20] A central role in liver injury, NASH, and fibrogenesis was demonstrated for NLRP3 inflammasome-dependent cleavage of caspase 1 and IL-1β.[9,10,13,23-25] Similarly, TNF-α was shown to be a key modulator in both liver inflammation and fibrosis.[7] Pyroptotic cell death, a caspase 1-dependent programmed form of cell death, is known to be crucial in the development of liver inflammation and fibrosis.[8,13,16] Clearly the progression from chronic inflammation to liver fibrogenesis is determined by a dynamic interplay between immune and nonimmune cells, and both recruited and resident cells. Notably, IL-1β and TNF-α are 2 key mediators of the intercellular crosstalk between immune cells and HSCs in liver fibrosis.[26] Therefore, revealing the cell-specific contribution of NLRP3 expression in the development of NASH and fibrogenesis is essential to understanding the complexity of disease pathogenesis and to design more rationale therapeutic approaches.

Previous studies had limited ability to investigate the cell-specific functions of NLRP3 in vivo in the context of acute and chronic models of liver injury. Our development of a conditional *Nlrp3* knock-out murine model removed the constraints of previous investigations. Using this novel model, our study demonstrated that myeloid-derived cells are the key cell type that drives inflammation in an acute model of liver injury induced via intraperitoneal injection of LPS and ATP. Deletion of NLRP3 in myeloid-derived cells had a profound effect of suppressing the increase in systemic and hepatic IL-1β levels induced by these stimuli as well as decreased inflammatory cell infiltration to the liver. Ablation of NLRP3 in hepatocytes showed a decrease in the mRNA levels of IL-1β but no effect on pro-cytokine or mature protein. In contrast, HSC-specific knockout of NLRP3 showed no effect in modulating the systemic and hepatic inflammatory changes. These results suggest that NLRP3 expressed in hepatocytes may have an indirect signal amplifying role as part of the feed-forward loop, initiated by hepatic myeloid cells, that results in further upregulation of NLRP3-related genes following exposure to danger signals.

Limited information is currently available regarding the contribution of cell-specific NLRP3 modulation during chronic liver injury, particularly in the context of NAFLD/NASH. Growing evidence points to a role for the NLRP3 inflammasome complex in NASH pathogenesis, as demonstrated by increased expression of the various components of the NLRP3 inflammasome in the livers of both human and murine NASH, studies employing various dietary models of NASH in global *Nlrp3* knockout mice, and studies using a selective NLRP3 small molecule inhibitor.[4,8,10,16,23] Additionally, previous studies using in vitro approaches have suggested that exposure of hepatocytes to lipotoxic lipids in association with LPS as a priming stressor can trigger NLRP3 activation.[16,27] Our group has previously reported that human and murine HSC express all components of the NLRP3 inflammasome, and stimulation with common NLRP3 activation stimuli results in a trans-differentiation of quiescent HSC into activated myofibroblasts and production of collagen.[14]

In the current study, we found that myeloid-derived cells are the predominant cell type that drives inflammation, fibrogenesis, and fibrotic changes in the CDAA-HFAT model of fibrotic NASH. *Nlrp3* deletion in myeloid-derived cells decreased programmed cell death in the liver, hepatic and systemic levels of pro-inflammatory cytokines, and neutrophil infiltration to the liver induced by this diet. Furthermore, myeloid-selective deletion decreased HSC activation and ameliorated liver fibrosis. However, HSC and hepatocyte specific *Nlrp3* deletion do not have a significant impact on the inflammatory events in NASH. Fibrogenesis was also not affected by HSC-specific NLRP3 deletion but partly reduced by hepatocyte-specific NLRP3 ablation, although in most instances, the changes did not reach statistical significance. To exclude that our findings were model-specific, we additionally completed a second model in a Western-type diet-induced NASH that validated our results showing that myeloid-specific Nlrp3 knock-out mice had decreased HSC activation and collagen deposition compared with controls. Thus, these results identify myeloid cells as the crucial cell type for NLRP3 inflammasome-mediated inflammation and fibrogenesis in murine NASH.

The interplay and crosstalk between recruited and resident cells are crucial in the setting of chronic inflammation.[3,17] In particular, neutrophils have been shown to influence cellular function and phenotype.[18] Our results showed that neutrophil and pro-inflammatory monocyte infiltration to the liver during NASH development in the CDAA-HFAT model depends on NLRP3 expression in myeloid cells, but not hepatocytes or HSCs. Both liver macrophages and neutrophils are crucial cells during acute and chronic liver inflammation and fibrogenesis. Through intercellular crosstalk between immune and nonimmune cells, these myeloid cells promote HSC activation and fibrosis.[26,28] NLRP3 deletion and inhibition in both resident (Kupffer cells) and infiltrating macrophages inhibit pathways that promote NASH development.[29-33] In this study,

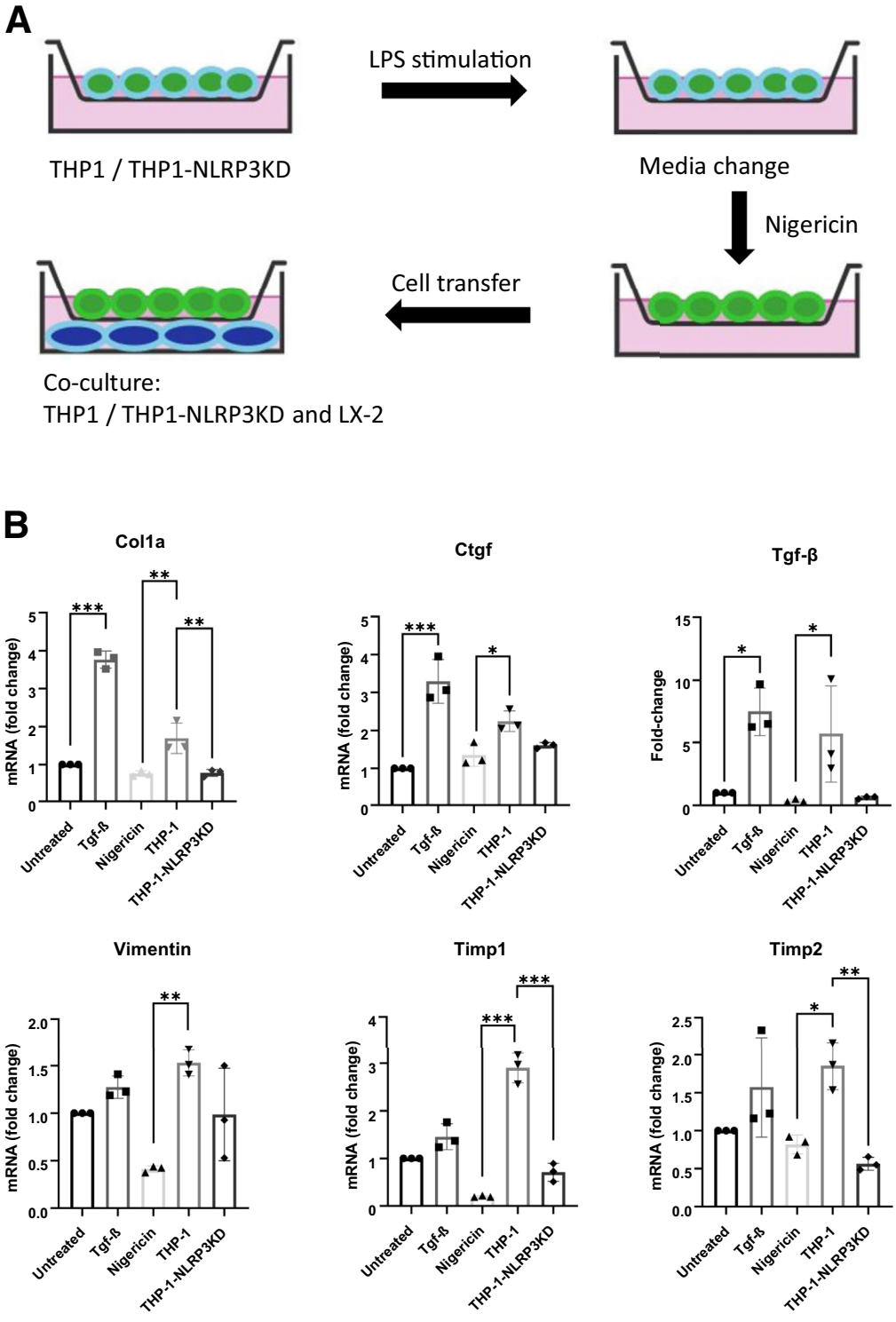


**Figure 8. NLRP3 activation in monocytes modulates transdifferentiation of HSCs into myofibroblast in co-cultured in vitro studies.** *A*, THP-1 or THP-1-NLRP3KD were grown in cell culture inserts and stimulated with LPS and nigericin or nigericin alone. After stimulation, THP-1 or THP-1-NLRP3KD and LX-2 were co-cultured by placing inserts containing THP-1 or THP-1-NLRP3KD in wells containing LX-2 cells at the bottom. *B*, Gene expression of *Col1a*, *Ctgf*, *Tgf-β*, *Timp1*, *Timp2*, and vimentin in LX-2 after cell stimulation with TGF-β, nigericin, NLRP3 inflammasome-activated THP-1, or THP-1-NLRP3KD. Expression of untreated LX-2 cells set as 1 (n = 3).

we showed that stimulation of the NLRP3 inflammasome in monocytes promotes subsequent activation of HSCs via in vitro co-cultures. These data support a crosstalk between leukocytes and HSCs contributing to the activation of HSCs into myofibroblast collagen producing cells, a central step in the development of fibrosis during NASH. Mice infected with *Schistosoma japonicum* or subjected to liver injury by bile duct ligation revealed high NLRP3 inflammasome activation in Kupffer cells and bone marrow-derived macrophages that enhanced fibrogenic mechanisms more than direct NLRP3 activation in HSCs.[34,35] In addition, NLRP3 inflammasome activation in Kupffer cells is known to mediate IL-1β-

dependent hepatocyte lipid accumulation, glucose output, and insulin sensitivity, and to aggravate NLRP3 inflammasome activation in hepatocytes.[36] Future studies to dissect the specific role of NLRP3 activation in liver macrophages vs neutrophils in vivo in the development of NASH-associated liver injury are warranted.

Taken together, the results of the current study reveal that NLRP3 inflammasome complex activation in myeloid cells is crucial for both pro-inflammatory and pro-fibrotic cytokine release and the development of liver inflammation and fibrosis induced by a CDAA-HFAT model of fibrotic NASH. Furthermore, human HSC can be activated by inflammasome induction in monocytes. These findings provide new insights in the cell-specific role of NLRP3 in NASH and may help to develop novel cell-specific strategies for NASH treatment.

## Materials and Methods

### Cell Lines

Human immortalized monocyte cells (THP-1) were purchased from the American Type Culture Collection (Manasass, VA; catalog code: tib-202) and THP-1-NLRP3KD from InvivoGen (THP-1-defNLRP3; catalog code: thp-dnlp), and cultured under conditions recommended by the manufacturer. Human immortalized HSCs (LX-2) were kindly provided by Prof Scott Friedman; they were maintained in Dulbecco's Modified Eagle Medium supplemented with 1% fetal bovine serum, 50 IU/mL penicillin, and 50 $\mu$g/mL streptomycin, at 37 °C in a humidified 5% $CO_2$ incubator.

### Mouse Strains

To investigate the cell-specific role of NLRP3 in liver diseases, a *Nlrp3* conditional knockout mouse model was generated. Exon 4 of murine *Nlrp3* was targeted for the conditional knockout. Deletion of this region results in the loss of function of mouse *Nlrp3* gene. First, a linearized vector was engineered. Mouse genomic fragments containing homology arms and conditional knockout region were generated and amplified from Bacterial Artificial Chromosome clone and sequentially assembled into a targeting vector together with recombination sites and selection markers (Figure 1). In the targeting vector, the Neo cassette was flanked by self-deletion anchor sites. Diphtheria toxin A was used for negative selection. The linearized vector was transfected into C57BL/6 embryonic stem cells that were then injected into C57BL/6 embryos, and finally reimplanted into CD-1 pseudo-pregnant females. Founder animals were identified by their coat color, and their germline transmission was confirmed by breeding with C57BL/6 females with subsequent genotyping of the offspring (Cyagen Biomodels LLC, Santa Clara, CA). Ultimately, the knockout allele is obtained after Cre-mediated recombination with cell-specific Cre mice. In this study, conditional *Nlrp3* knockout mice were bred to mice expressing Cre recombinase under control of Alb (hepatocyte-specific knockout of *Nlrp3*, obtained from The Jackson Laboratory, Jax #003574, B6.Cg-Speer6-ps1$^{Tg(Alb\text{-}cre)21Mgn}$/J), Lyz (myeloid lineage specific knockout of *Nlrp3*, obtained from The Jackson Laboratory, Jax #004781, B6.129P2-Lyz2$^{tm1(cre)Ifo}$/J), and LRAT (hepatic stellate cell-specific knockout of *Nlrp3*, provided by Robert Schwabe, Columbia University, New York, NY). These mice are here referred to as *Nlrp3*$^{-/-}$*-Alb-cre (Alb)*, *Nlrp3*$^{-/-}$*-Lyz-cre (Lyz)* and *Nlrp3*$^{-/-}$*-LRAT-cre (LRAT)*, respectively. In addition, global NLRP3 knockout mice were used in this study (*Nlrp3*$^{-/-}$ (Global), provided by J. Bertin, E. Grant, A. Coyle, and Millennium Pharmaceuticals). Littermates lacking the Cre recombinase were used as control mice. The experimental protocols were approved by the Institutional Animal Care and Use Committee at the University of California, San Diego. All efforts were made to minimize pain and distress during animal husbandry and experimental assessments.

### CDAA-HFAT and Western Diet to Induce NASH Fibrosis

A CDAA-HFAT (Research Diets, New Brunswick, NJ) or choline-supplemented, L-amino acid-defined control diet was fed to mice for 10 weeks starting at the age of 8 weeks. As a second dietary NASH model, a Western diet (high fat, fructose and cholesterol diet and water supplemented with sucrose/fructose) (AIN-76A Western Diet, TestDiet, St. Louis, MO) or chow control diet was fed to mice for 20 weeks starting at the age of 8 weeks. For dietary experiments, groups (knock-outs and controls) were cohoused. Mice fed CDAA diet show severe NASH characterized by steatohepatitis and fibrosis.

### Cell Stimulation

THP-1 and THP-1-NLRP3KD were cultured in 1 $\mu$m pore-size cell culture inserts of 24-well plates (Falcon, catalog number: 353104), which allow diffusion of media components but prevent cell migration, and stimulated with 1 $\mu$g/mL LPS for 3 hours, followed by change of medium and treatment with 12.5 $\mu$M nigericin for 16 hours. Next, THP-1 or THP-1-NLRP3KD and LX-2 were co-cultured. Inserts containing $1 \times 10^5$ THP-1 or THP-1-NLRP3KD were placed in wells containing $1 \times 10^5$ LX-2 cells at the bottom (Dulbecco's Modified Eagle Medium; ThermoFisher Scientific, Waltham, MA). LX-2 cells were harvested 24 hours after co-culturing.

### LPS/ATP in vivo Model of Acute Liver and Systemic Inflammation

Mice were administered 1 $\mu$g of LPS (*Escherichia coli* O55:B5, Sigma-Aldrich, MO) in 0.5 phosphate buffered saline mL intraperitoneally. Two hours after the administration of LPS, the mice were injected intraperitoneally with 80 mM ATP (ATP disodium salt hydrate, Sigma-Aldrich, MO) in 0.5 mL PBS adjusted to 7.2 pH. 30 minutes after ATP injection, mice were euthanized via $CO_2$ inhalation and blood collected via heart puncture. Immediately after blood collection, the peritoneal cavity was lavaged with 3 mL ice-cold phosphate buffered saline containing 25 U/mL heparin (heparin sodium salt from porcine intestinal mucosa, Sigma-

Aldrich, MO), cOmplete ULTRA Tablets protease inhibitor cocktail (Roche, Switzerland) and 10% fetal bovine serum. Approximately 2 mL of the lavage fluid was centrifuged to remove cells and debris and stored at −80 °C for subsequent determination of IL-1$\beta$ concentrations.

### Liver Sample Preparation

Mice were sacrificed at the terminal end point of each experiment (30 minutes after ATP injection/at the end of the feeding cycles). Mice were anesthetized, and liver tissue was harvested as follows: (1) a representative section was fixed in 10% formalin for 24 hours and embedded in paraffin; (2) a representative section was embedded in OCT for frozen tissue sections; (3) samples of 50 $\mu$g were placed in 0.5 mL of RNAlater Solution (Lifetechnologies, Carlsbad, CA); (4) remaining liver tissue was quickly frozen in liquid nitrogen and stored at −80 °C.

### Liver Function Test

Blood samples were collected at the terminal end point of each experiment (30 minutes after ATP injection/at the end of the feeding cycles), and serum values of ALT were measured according to the manufacturer's instruction (Infinity ALT, ThermoFisher Scientific, Waltham, MA).

### ELISA

Values of IL-1$\beta$ in serum and peritoneal lavage were measured by ELISA according to the manufacturer's instruction using the DuoSet ELISA kit (R&D, Cat. No DY401-05).

### Liver Histology, Immunostaining, and Sirius Red Staining

Paraffin-embedded liver tissues were stained for H&E. For the assessment of liver fibrosis, Sirius Red staining was performed. Briefly, liver sections were incubated for 1 hour at room temperature with an aqueous solution of saturated picric acid containing 0.1% Direct Red (Sirius Red). Immunohistochemistry staining for lymphocyte antigen 6 complex, locus G (Ly6G, ThermoFisher Scientific, Waltham, MA), lymphocyte antigen 6 complex, locus C1 (Ly6C, Abcam, Cambridge, MA), $\alpha$-SMA ($\alpha$-SMA, Abcam, Cambridge, MA), CD11b (Abcam, Cambridge, MA), and F4/80 (F4/80, BioLegend, San Diego, CA) was performed on formalin-fixed, paraffin-embedded liver sections. After specimens were deparaffinized and hydrated in ethanol, Proteinase K was applied at room temperature (Ready-to use Proteinase K, Dako, Agilent Technologies, Santa Clara, CA) followed by blocking with 3% bovine serum albumin (BSA) in TBS-T for 1 hour at room temperature (Ly6G, Ly6C), treated with 2% BSA 1× Triton for 30 minutes at room temperature followed by blocking with 1% BSA in TBS-T for 10 minutes at room temperature ($\alpha$-SMA, F4/80) or treated with citrate buffer at 95 °C for 20 minutes (CD11b). After overnight incubation with primary antibodies, respective secondary antibodies were applied, and color reaction was performed with a streptavidin-peroxidase complex, using 3,3-diaminobenzidine tetrahydrochloride. Slides were counterstained with hematoxylin. Apoptosis was assessed by TUNEL assay according to the manufacturer's instructions (ApopTag Peroxidase In Situ Apoptosis Detection Kit, Millipore, Billerica, MA). Images of all histologic sections were taken by NanoZoomer 2.0HT Slide Scanning System (Hamamatsu, Japan). The number of positive cells per field or positive stained areas for Ly6G, Ly6C, $\alpha$-SMA, Sirius Red, CD11b, and F4/80 staining were quantified using ImageJ software (Version 1.52a, Nationals Institute of Health, Bethesda, MD).

### Immunoblot Analysis

For protein extraction, whole liver tissue was homogenized in radioimmunoprecipitation assay buffer (Cell Signaling, Danvers, MA) together with cocktails of protease and phosphatase inhibitors (Sigma-Aldrich, St. Louis, MO). For immunoblot analysis, 30 $\mu$g of protein lysate was resolved on Any kD Criterion TGX Precast Gels (Biorad, Hercules, CA), transferred to nitrocellulose membrane, and blocked with Intercept Blocking Buffer (LI-COR, Lincoln, NE) for 1 hour before being incubated with primary antibodies overnight at 4 °C. Membranes were incubated with IRDye secondary antibody (LI-COR, Lincoln, NE), and protein bands were visualized with LI-COR Imaging System (LI-COR, Lincoln, NE). Expression intensity was quantified by Image Studio Licor (LI-COR, Lincoln, NE). Protein load was verified with anti-$\beta$-Actin antibody. Anti-IL-1$\beta$ (Abcam, Cambridge, UK; 1:500), anti-caspase-1 (Santa Cruz, CA; 1:500), anti-TNF-$\alpha$ (Cell Signaling, Danvers, MA; 1;500), anti-type 1 collagen (Birmingham, AL; 1:500), anti-$\alpha$-SMA (Abcam, Cambridge, UK; 1:500), and anti-$\beta$-actin (Millipore/Sigma, Burlington, MA; 1:6000) were used.

### Real-time PCR

RNA was isolated from cells and liver tissue using the RNeasy Tissue Mini kit according to manufacturer's instructions (Qiagen, Valencia, CA, USA). Complementary DNA was synthesized from 1 $\mu$g of total RNA using the qScript cDNA SuperMix according to manufacturer's instructions (Beverly, MA). Real-time PCR quantification was performed using TaqMan Fast Advanced Master Mix (ThermoFisher Scientific, Vilnius, Lithuania). Briefly, 20 $\mu$l of reaction mix contained cDNA, TaqMan Fast Advanced Master Mix, and respective primers. Primers were purchased from ThermoFisher Scientific (Waltham, MA). Assay IDs for the primers are listed in Table 1. QuantStudio Design Software (ThermoFisher Scientific, Waltham, MA) was used for analyses.

### Statistical Analyses

Analyses were performed with GraphPad (version 8.4.2; Graph Pad Software Inc, La Jolla, CA, USA). Analysis of variance followed by Tukey's multiple comparison was used to analyze 3 or more groups. The significance level was set at $P < .05$ for all comparisons ($^*P < .05$; $^{**}P < .01$; $^{***}P < .001$; unless otherwise stated). Unless otherwise stated, data are expressed as mean ± standard deviation or as percentage for categorical variables.

**Table 1.** Assay ID of Primers Used for qPCR

| | |
|---|---|
| Murine | |
| Acta2/$\alpha$-SMA | Mm00725412_s1 |
| Adgre1 - F4/80 | Mm00802529_m1 |
| Col1a | Mm00801666_g1 |
| Col3a | Mm01254476_m1 |
| Ctgf | Mm01192933_g1 |
| Cxcl1 | Mm04207460_m1 |
| Cxcl2 | Mm00436450_m1 |
| Gapdh | Mm99999915_g1 |
| Il1b | Mm00434228_m1 |
| Ly6C | Mm03009946_m1 |
| Ly6G | Mm04934123_m1 |
| Mmp2 | Mm00439498_m1 |
| Nlrp3 | Mm00840904_m1 |
| Tgf-$\beta$ | Mm01178820_m1 |
| Timp1 | Mm01341361_m1 |
| Vimentin | Mm01333430_m1 |
| Human | |
| Col1a | Hs00164004_m1 |
| Ctgf | Hs00170014_m1 |
| Gapdh | Hs99999905_m1 |
| Tgf-$\beta$ | Hs00998133_m1 |
| Timp1 | Hs01092512_g1 |
| Timp2 | Hs00234278_m1 |
| Vimentin | Hs00958111_m1 |

qPCR, Quantitative polymerase chain reaction.

## References


1. AYounossi Z, Anstee QM, Marietti M, Hardy T, Henry L, Eslam M, George J, Bugianesi E. Global burden of NAFLD and NASH: trends, predictions, risk factors and prevention. Nat Rev Gastroenterol Hepatol 2018; 15:11–20.
2. Marengo A, Jouness RI, Bugianesi E. Progression and natural history of nonalcoholic fatty liver disease in adults. Clin Liver Dis 2016;20:313–324.
3. Schuster S, Cabrera D, Arrese M, Feldstein AE. Triggering and resolution of inflammation in NASH. Nat Rev Gastroenterol Hepatol 2018;15:349–364.
4. Mridha AR, Wree A, Robertson AAB, Yeh MM, Johnson CD, Van Rooyen DM, Haczeyni F, Teoh NC, Savard C, Ioannou GN, Masters SL, Schroder K, Cooper MA, Feldstein AE, Farrell GC. NLRP3 inflammasome blockade reduces liver inflammation and fibrosis in experimental NASH in mice. J Hepatol 2017; 66:1037–1046.
5. Wan X, Xu C, Yu C, Li Y. Role of NLRP3 inflammasome in the progression of NAFLD to NASH. Can J Gastroenterol Hepatol 2016;2016:6489012.
6. Szabo G, Csak T. Inflammasomes in liver diseases. J Hepatol 2012;57:642–654.
7. Wree A, McGeough MD, Inzaugarat ME, Eguchi A, Schuster S, Johnson CD, Peña CA, Geisler LJ, Papouchado BG, Hoffman HM, Feldstein AE. NLRP3 inflammasome-driven liver injury and fibrosis: roles of IL-17 and TNF in mice. Hepatology 2018; 67:736–749.
8. Wree A, McGeough MD, Peña CA, Schlattjan M, Li H, Inzaugarat ME, Messer K, Canbay A, Hoffman HM, Feldstein AE. NLRP3 inflammasome activation is required for fibrosis development in NAFLD. J Mol Medicine (Berl) 2014;92:1069–1082.
9. Kamari Y, Shaish A, Vax E, Shemesh S, Kandel-Kfir M, Arbel Y, Olteanu S, Barshack I, Dotan S, Voronov E, Dinarello CA, Apte RN, Harats D. Lack of interleukin-1$\alpha$ or interleukin-1$\beta$ inhibits transformation of steatosis to steatohepatitis and liver fibrosis in hypercholesterolemic mice. J Hepatol 2011;55:1086–1094.
10. Dixon LJ, Berk M, Thapaliya S, Papouchado BG, Feldstein AE. Caspase-1-mediated regulation of fibrogenesis in diet-induced steatohepatitis. Lab Invest 2012; 92:713–723.
11. Knorr J, Wree A, Tacke F, Feldstein AE. The NLRP3 inflammasome in alcoholic and nonalcoholic steatohepatitis. Semin Liver Dis 2020;40:298–306.
12. Alegre F, Pelegrin P, Feldstein AE. Inflammasomes in liver fibrosis. Semin Liver Dis 2017;37:119–127.
13. Wree A, Eguchi A, McGeough MD, Pena CA, Johnson CD, Canbay A, Hoffman HM, Feldstein AE. NLRP3 inflammasome activation results in hepatocyte pyroptosis, liver inflammation, and fibrosis in mice. Hepatology 2014;59:898–910.
14. Inzaugarat ME, Johnson CD, Holtmann TM, McGeough MD, Trautwein C, Papouchado BG, Schwabe R, Hoffman HM, Wree A, Feldstein AE. NLR family pyrin domain-containing 3 inflammasome activation in hepatic stellate cells induces liver fibrosis in mice. Hepatology 2019;69:845–859.
15. Watanabe A, Sohail MA, Gomes DA, Hashmi A, Nagata J, Sutterwala FS, Mahmood S, Jhandier MN, Shi Y, Flavell RA, Mehal WZ. Inflammasome-mediated regulation of hepatic stellate cells. Am J Physiol Gastrointest Liver Physiol 2009;296:G1248–G1257.
16. Gaul S, Leszczynska A, Alegre F, Kaufmann B, Johnson CD, Adams LA, Wree A, Damm G, Seehofer D, Calvente CJ, Povero D, Kisseleva T, Eguchi A, McGeough MD, Hoffman HM, Pelegrin P, Laufs U, Feldstein AE. Hepatocyte pyroptosis and release of inflammasome particles induce stellate cell activation and liver fibrosis. J Hepatol 2021;74:156–167.
17. Benetti E, Chiazza F, Patel NS, Collino M. The NLRP3 inflammasome as a novel player of the intercellular crosstalk in metabolic disorders. Mediators Inflamm 2013;2013:678627.
18. Soehnlein O, Steffens S, Hidalgo A, Weber C. Neutrophils as protagonists and targets in chronic inflammation. Nat Rev Immunol 2017;17:248–261.
19. Wu KK, Cheung SW, Cheng KK. NLRP3 inflammasome activation in adipose tissues and its implications on metabolic diseases. Int J Mol Sci 2020;21:4184.
20. Szabo G, Petrasek J. Inflammasome activation and function in liver disease. Nat Rev Gastroenterol Hepatol 2015;12:387–400.
21. Griffiths RJ, Stam EJ, Downs JT, Otterness IG. ATP induces the release of IL-1 from LPS-primed cells in vivo. J Immunol 1995;154:2821–2828.
22. Wree A, Holtmann TM, Inzaugarat ME, Feldstein AE. Novel drivers of the inflammatory response in liver injury and fibrosis. Semin Liver Dis 2019;39:275–282.

23. Dixon LJ, Flask CA, Papouchado BG, Feldstein AE, Nagy LE. Caspase-1 as a central regulator of high fat diet-induced non-alcoholic steatohepatitis. PLoS One 2013;8:e56100.
24. Petrasek J, Bala S, Csak T, Lippai D, Kodys K, Menashy V, Barrieau M, Min SY, Kurt-Jones EA, Szabo G. IL-1 receptor antagonist ameliorates inflammasome-dependent alcoholic steatohepatitis in mice. J Clin Invest 2012;122:3476–3489.
25. Gieling RG, Wallace K, Han YP. Interleukin-1 participates in the progression from liver injury to fibrosis. Am J Physiol Gastrointest Liver Physiol 2009;296:G1324–G1331.
26. Seki E, Schwabe RF. Hepatic inflammation and fibrosis: functional links and key pathways. Hepatology 2015; 61:1066–1079.
27. Csak T, Ganz M, Pespisa J, Kodys K, Dolganiuc A, Szabo G. Fatty acid and endotoxin activate inflammasomes in mouse hepatocytes that release danger signals to stimulate immune cells. Hepatology 2011;54:133–144.
28. Krenkel O, Tacke F. Liver macrophages in tissue homeostasis and disease. Nat Rev Immunol 2017; 17:306–321.
29. Yang ZY, Liu F, Liu PH, Guo WJ, Xiong GY, Pan H, Wei L. Obeticholic acid improves hepatic steatosis and inflammation by inhibiting NLRP3 inflammasome activation. Int J Clin Exp Pathol 2017;10:8119–8129.
30. Cai C, Zhu X, Li P, Li J, Gong J, Shen W, He K. NLRP3 deletion inhibits the non-alcoholic steatohepatitis development and inflammation in Kupffer cells induced by palmitic acid. Inflammation 2017;40:1875–1883.
31. He K, Zhu X, Liu Y, Miao C, Wang T, Li P, Zhao L, Chen Y, Gong J, Cai C, Li J, Li S, Ruan XZ, Gong J. Inhibition of NLRP3 inflammasome by thioredoxin-interacting protein in mouse Kupffer cells as a regulatory mechanism for non-alcoholic fatty liver disease development. Oncotarget 2017;8:37657–37672.
32. Huang S, Wu Y, Zhao Z, Wu B, Sun K, Wang H, Qin L, Bai F, Leng Y, Tang W. A new mechanism of obeticholic acid on NASH treatment by inhibiting NLRP3 inflammasome activation in macrophage. Metabolism 2021;120:154797.
33. Pan J, Ou Z, Cai C, Li P, Gong J, Ruan XZ, He K. Fatty acid activates NLRP3 inflammasomes in mouse Kupffer cells through mitochondrial DNA release. Cell Immunol 2018;332:111–120.
34. Zhang WJ, Fang ZM, Liu WQ. (2019). NLRP3 inflammasome activation from Kupffer cells is involved in liver fibrosis of Schistosoma japonicum-infected mice via NF-κB. Parasit Vectors 2019;12:29.
35. Hou L, Yang L, Chang N, Zhao X, Zhou X, Dong C, Liu F, Yang L, Li L. Macrophage sphingosine 1-phosphate receptor 2 blockade attenuates liver inflammation and fibrogenesis triggered by NLRP3 inflammasome. Front Immunol 2020;11:1149.
36. Zheng T, Wang Q, Dong Y, Ma W, Zhang Y, Zhao Y, Bian F, Chen L. High glucose-aggravated hepatic insulin resistance: role of the NLRP3 inflammasome in Kupffer xells. Obesity (Silver Spring) 2020;28:1270–1282.

**Correspondence**
Address correspondence to: Dr Ariel E. Feldstein, Professor of Pediatrics, UC San Diego, 3020 Children's Way, MC 5030, San Diego, CA 92103-8450. e-mail: afeldstein@ucsd.edu; tel: (858) 966-8907.

**CRediT Authorship Contributions**

Benedikt Kaufmann (Conceptualization: Lead; Data curation: Lead; Formal analysis: Lead; Funding acquisition: Lead; Investigation: Lead; Methodology: Lead; Writing – original draft: Lead)

Lin Kui (Data curation: Supporting; Formal analysis: Supporting; Writing – review & editing: Supporting)

Agustina Reca (Data curation: Supporting; Investigation: Supporting; Writing – original draft: Supporting)

Aleksandra Leszczynska (Data curation: Supporting; Formal analysis: Supporting; Investigation: Supporting)

Andrea D. Kim (Data curation: Supporting; Methodology: Supporting)

Laela M. Booshehri (Data curation: Supporting; Methodology: Supporting)

Alexander Wree (Supervision: Supporting; Writing – review & editing: Supporting)

Helmut Friess (Supervision: Supporting; Writing – review & editing: Supporting)

Daniel Hartmann (Supervision: Supporting; Writing – review & editing: Supporting)

Lori Broderick (Conceptualization: Equal; Funding acquisition: Equal; Resources: Equal; Supervision: Equal; Writing – original draft: Equal)

Hal M. Hoffman (Conceptualization: Equal; Funding acquisition: Equal; Project administration: Equal; Resources: Equal; Supervision: Equal; Writing – original draft: Equal)

Ariel E. Feldstein (Conceptualization: Lead; Funding acquisition: Lead; Project administration: Lead; Supervision: Lead; Writing – original draft: Equal)

**Conflicts of interest**
These authors disclose the following: Lori Broderick is a site Principal Investigator for Novartis, Inc. Hal M. Hoffman is a consultant for Novartis and has research collaborations with Jecure, Inc, Zomagen, Inc, and Takeda, Inc. Ariel E. Feldstein is consultant for Ventyx Bio, Inc, Novo Nordisk, and Inipharm and has research collaborations with Takeda, Inc. The remaining authors disclose no conflicts.

**Funding**
This work was funded by National Institutes of Health grants R01 DK113592, R01 AA024206 to Ariel E. Feldstein, Hal M. Hoffman, and Lori Broderick; and German Research Foundation (DFG-Grant KA 5089/1-1) to Benedikt Kaufmann.